Pharmacological Research 151 (2020) 104548

Contents lists available at ScienceDirect

Pharmacological Research

journal homepage: www.elsevier.com/locate/yphrs

A novel class of cardioprotective small-molecule PTP inhibitors

Salvatore Antonucci[a,1], Moises Di Sante[a,1], Justina Sileikyte[b,1], Jordan Deveraux[b], Tyler Bauer[c], Michael J. Bround[d], Roberta Menabò[a,e], Melanie Paillard[f], Petra Alanova[a,g], Michela Carraro[a], Michel Ovize[f], Jeffery D. Molkentin[d,h], Michael Cohen[b], Michael A. Forte[b], Paolo Bernardi[a,e], Fabio Di Lisa[a,e,*], Elizabeth Murphy[c,**]

[a] Department of Biomedical Sciences, University of Padova, Padova, Italy
[b] Vollum Institute, and Department of Physiology and Pharmacology, Portland, OR, USA
[c] Systems Biology Center, NHLBI, NIH, Bethesda, MD, USA
[d] Department of Pediatrics, Cincinnati Children's Hospital Medical Center, University of Cincinnati, Cincinnati, OH, USA
[e] National Research Council of Italy (CNR), Padova, Italy
[f] CarMeN Laboratory, University Claude Bernard Lyon 1, INSA Lyon, Oullins, France
[g] Department of Developmental Cardiology, Institute of Physiology CAS, Prague, Czech Republic
[h] Howard Hughes Medical Institute, Cincinnati Children's Hospital Medical Center, Cincinnati, OH, USA

ARTICLE INFO

Chemical compounds studied in this article:
Caffeine (PubChem CID: 2519)
Calcimycin (PubChem CID: 40486)
Compound 63 (PubChem CID: 75204518)
Cyclosporine A (PubChem CID: 5284373)
MitoParaquat (PubChem CID: 129909777)

Keywords:
Permeability transition
Mitochondria
Cardiomyocytes
Cardioprotection
Ischemia
Reperfusion

ABSTRACT

Ischemia/reperfusion (I/R) injury is mediated in large part by opening of the mitochondrial permeability transition pore (PTP). Consequently, inhibitors of the PTP hold great promise for the treatment of a variety of cardiovascular disorders. At present, PTP inhibition is obtained only through the use of drugs (e.g. cyclosporine A, CsA) targeting cyclophilin D (CyPD) which is a key modulator, but not a structural component of the PTP. This limitation might explain controversial findings in clinical studies. Therefore, we investigated the protective effects against I/R injury of small-molecule inhibitors of the PTP (63 and TR002) that do not target CyPD. Both compounds exhibited a dose-dependent inhibition of PTP opening in isolated mitochondria and were more potent than CsA. Notably, PTP inhibition was observed also in mitochondria devoid of CyPD. Compounds 63 and TR002 prevented PTP opening and mitochondrial depolarization induced by Ca^{2+} overload and by reactive oxygen species in neonatal rat ventricular myocytes (NRVMs). Remarkably, both compounds prevented cell death, contractile dysfunction and sarcomeric derangement induced by anoxia/reoxygenation injury in NRVMs at sub-micromolar concentrations, and were more potent than CsA. Cardioprotection was observed also in adult mouse ventricular myocytes and human iPSc-derived cardiomyocytes, as well as *ex vivo* in perfused hearts. Thus, this study demonstrates that 63 and TR002 represent novel cardioprotective agents that inhibit PTP opening independent of CyPD targeting.

1. Introduction

Cardiovascular diseases remain the leading cause of death worldwide, mainly due to acute myocardial infarction (MI) [1]. No therapeutic strategy is yet available to both reduce infarct size following ischemia and reperfusion, and to mitigate the risk of developing heart failure. Indeed, ischemia/reperfusion (I/R) injury is thought to play a major role in cell death after MI. Therefore, targeting pathways that lead to I/R injury are potential clinical targets that could significantly curtail the size and severity of myocardial injury following acute MI.

One causative event of I/R injury is opening of the permeability transition pore (PTP). The PTP is a regulated, transmembrane pore of the inner mitochondrial membrane which allows permeation of solutes up to 1.5 kDa. Classically, PTP activation can be triggered by Ca^{2+}

Abbreviations: A/R, anoxia/reoxygenation; AMVMs, adult mouse ventricular myocytes; CRC, calcium retention capacity; CsA, cyclosporine A; CyPD, cyclophilin D; hiPSc-CMs, human iPSc-derived cardiomyocytes; I/R, ischemia/reperfusion; LDH, lactate dehydrogenase; MI, myocardial infarction; MitoPQ, MitoParaquat; NRVMs, neonatal rat ventricular myocytes; PTP, permeability transition pore; ROS, reactive oxygen species; TMRM, tetramethylrhodamine; $\Delta\Psi m$, mitochondrial membrane potential

* Corresponding author at: Department of Biomedical Sciences, University of Padova, Padova, Italy.
** Corresponding author at: Systems Biology Center, NHLBI, NIH, Bethesda, MD, USA.
E-mail addresses: dilisa@bio.unipd.it (F. Di Lisa), murphy1@nhlbi.nih.gov (E. Murphy).
[1] These authors contributed equally to this work.

https://doi.org/10.1016/j.phrs.2019.104548
Received 8 September 2019; Received in revised form 12 November 2019; Accepted 14 November 2019
Available online 20 November 2019

overload and reactive oxygen species (ROS), while PTP opening can be blocked by other divalent cations, ADP and low matrix pH [2,3]. PTP opening leads to mitochondrial depolarization, swelling, and respiratory inhibition which initiates cell death in cardiac cells [4,5]. Many studies have explored the PTP as a potential drug target in cardioprotection [6–9]. These studies focused on the use of cyclosporine A (CsA), a cyclophilin D (CyPD)-binding cyclic peptide [10], as an inhibitor of the PTP because CyPD is a known regulator of the PTP. Indeed, CsA reduces infarct size in multiple preclinical models of cardiovascular disease [6,11]. However, phase III clinical trials demonstrated that CsA provided no benefit for patients presenting with acute MI [12,13]. While it is not clear why CsA failed in phase III clinical trials for acute MI, it is worth noting that CsA is not a direct inhibitor of the PTP. Thus, there is a critical need for selective PTP inhibitors in order to determine the therapeutic potential of targeting the PTP in acute MI and to elucidate the mechanisms by which the PTP contributes to I/R injury.

Recently, we have used a combination of high throughput screening and follow-up medicinal chemistry to discover novel small-molecule inhibitors of the PTP [14–16]. The most potent inhibitors are based on an isoxazole or triazole scaffold. These compounds prevented PTP opening in mouse liver mitochondria in a CyPD-independent manner, suggesting that they act via a novel mechanism—perhaps by directly targeting the PTP. The triazole-based variants showed improved plasma stability compared to the isoxazole-based inhibitors, and were particularly efficacious in a zebrafish model of collagen VI muscular dystrophy, which is characterized by PTP deregulation and chronic mitochondrial dysfunction [16]. Here, we tested the potential cardioprotective effects of two compounds in this series, the isoxazole 63 [14] and the structurally-related triazole analogue TR002 [16]. Our results indicate that targeting the PTP with small-molecule inhibitors independent of CyPD can protect cardiac mitochondria, cells, and tissue from I/R-induced cardiac injury.

2. Results

2.1. 63 and TR002 prevent PTP opening in isolated cardiac mitochondria

Small-molecule isoxazole (63) and triazole (TR002) compounds (Fig. 1A) are novel, potent inhibitors of the PTP that were identified and optimized following the screen of NIH MLPCN collection of 362,000 compounds [14] using mouse liver mitochondria. We assessed the ability of these inhibitors to desensitize the PTP in isolated heart mitochondria using a Ca^{2+} retention capacity (CRC) assay. CRC measures the Ca^{2+} load needed for PTP opening, which is marked by a sudden release of the previously accumulated cation. Mitochondrial suspensions were incubated with 1 μM 63, TR002 or CsA and subsequently challenged with a train of 10 μM Ca^{2+} pulses. Compared to CsA, we found that 63 and TR002 more effectively increased the threshold Ca^{2+} required for PTP opening (Fig. 1B). The CRC ratio was increased in a concentration-dependent manner for all three compounds, however, 63 was the most potent, followed by TR002 (Fig. 1C). At 10 μM TR002, we observed a decrease in the CRC ratio, suggesting that at this concentration TR002 may exhibit adverse effects (Fig. 1C); therefore, in all subsequent experiments we used concentrations of 1 μM or less for TR002. Taken together, these results demonstrate that 63 and TR002 were more effective inhibitors of the PTP than CsA in isolated heart mitochondria.

We previously showed that isoxazole and triazole-based PTP inhibitors structurally related to 63 and TR002 inhibited PTP opening in liver mitochondria and HEK293 cells in a CyPD-independent manner [16]. To confirm that 63 and TR002 function independently of CyPD in heart mitochondria, we conducted CRC and mitochondrial swelling assays on isolated heart mitochondria from wild type and *Ppif*$^{-/-}$ mice (Fig. 1D–G). We observed that 63, TR002, and CsA protected against PTP opening induced with a train of 5 μM Ca^{2+} pulses in wild type heart mitochondria (Fig. 1D–E). By contrast, 63 and TR002 provided additional protection against PTP opening in *Ppif*$^{-/-}$ heart mitochondria (Fig. 1F–G). These results were confirmed in liver mitochondria challenged with large boluses of Ca^{2+} (i.e. 100 μM) (Supplementary Fig. 1A–D). These results demonstrate that 63 and TR002 inhibit PTP independently of CyPD.

2.2. Compounds 63 and TR002 prevent PTP opening and mitochondrial membrane depolarization induced by calcium and ROS

We next investigated the effects of 63 and TR002 in intact cardiomyocytes. In these experiments, opening of the PTP was assessed in neonatal rat ventricular myocytes (NRVMs) by monitoring the decrease in calcein fluorescence [17]. NRVMs were pre-treated with DMSO, CsA, 63 or TR002, and PTP opening was induced by the Ca^{2+} ionophore calcimycin. Treatment with either 0.5 μM 63 or 0.5 μM TR002 delayed PTP opening (Fig. 2A). Notably, after 180 s of calcimycin treatment the decrease in calcein fluorescence was significantly lower compared to the DMSO control (DMSO: 71.9 ± 6.5 % vs 63: 25.5 ± 6.9 % or TR002: 33.9 ± 11.4 %, Fig. 2B).

PTP inhibition was reported to prevent mitochondrial depolarization and cardiomyocyte derangements induced by I/R [18,19]. To investigate whether 63 and TR002 could prevent such mitochondrial dysfunction, we monitored ΔΨm using tetramethylrhodamine (TMRM) fluorescence. NRVMs were pre-treated with 63, TR002, or CsA. Since CsA is also an inhibitor of the multidrug resistance P-glycoprotein (MDR), which may alter TMRM distribution, cells were also pre-treated with cyclosporine H which inhibits the MDR but does not affect PTP opening [20]. NRVMs treated with calcimycin displayed a decrease in ΔΨm (20 %) that was prevented by treatment with both 63 and TR002 (Fig. 2C–E). Then, to investigate the increased propensity to PTP opening caused by oxidative stress, we used MitoParaquat (MitoPQ), which induces a primary increase in mitochondrial ROS levels [21]. NRVMs were pre-treated with 1 μM MitoPQ and then exposed to Ca^{2+} overload by means of calcimycin in presence or absence of 63, TR002 or CsA. NRVMs treated with calcimycin and MitoPQ displayed a dramatic drop in ΔΨm (50 %) that was completely prevented by both 63 and TR002 (Fig. 2D–E). Taken together, these results demonstrate that compounds 63 and TR002 prevent PTP opening and the associated mitochondrial dysfunction induced by either Ca^{2+} or by the combination of Ca^{2+} overload and a selective increase in mitochondrial ROS levels.

2.3. Compounds 63 and TR002 prevent Ca^{2+} dysregulation and sarcomeric impairment in NRVMs following anoxia/reoxygenation

We next investigated if inhibition of PTP opening by 63 and TR002 could prevent alterations of intracellular [Ca^{2+}] homeostasis induced by anoxia and reoxygenation (A/R) in NRVMs. NRVMs were subjected to either 3 h or 6 h of anoxia followed by reoxygenation, and intracellular [Ca^{2+}] transients were monitored by means of Fluo-4 fluorescence during the reoxygenation phase. Upon reoxygenation after 3 h of anoxia the number of beating cells was significantly higher in the cells treated with 63 or TR002 compared to the control (DMSO: 22.8 ± 11.3 % vs 63: 83.3 ± 12.9 % or TR002: 80.0 ± 25.8 %, Fig. 3F). However, if one compares the beating cells, NRVMs treated with either 63 or TR002 did not display significant differences in Ca^{2+} transients compared to the anoxic control. Indeed, although NRVMs treated with the compounds exhibit an oscillatory pattern similar to the normoxic cells (Fig. 3A, Supplementary Fig. 2A), there were no differences in transient amplitude, in transient frequency and in response to caffeine (Fig. 3C–E). Interestingly, the ability of NRVMs to decrease the level of Ca^{2+} in the cytosolic compartment following caffeine addition, which releases Ca^{2+} from sarcoplasmic reticulum (SR), was lower in DMSO-treated cells than in cardiomyocytes treated with either 63 or TR002 (Supplementary Fig. 2B), especially after 6 h of anoxia. Moreover,

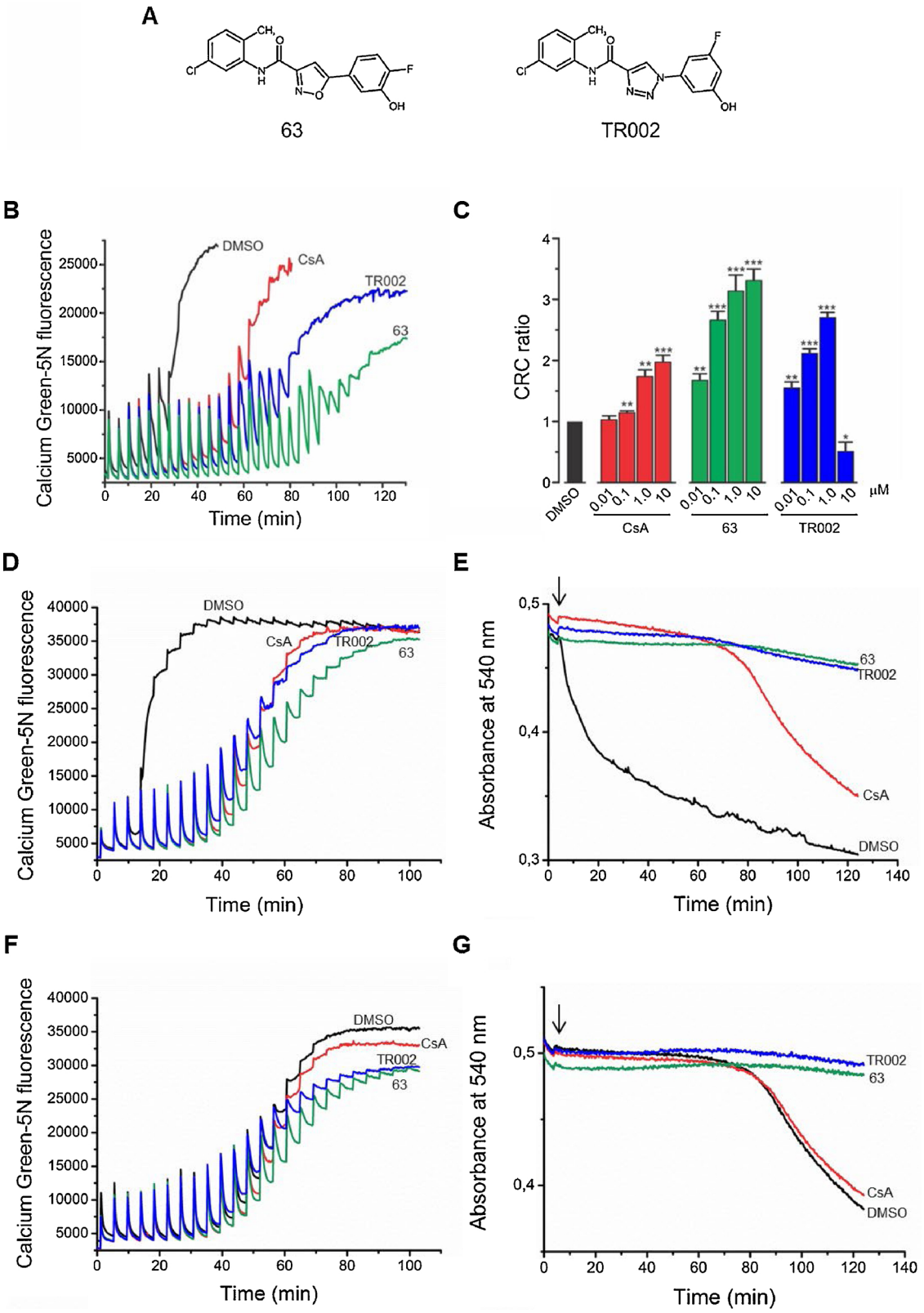

Fig. 1. Effects of compounds 63 and TR002 on PTP opening in isolated cardiac mitochondria. A) Chemical structures of the compounds 63 and TR002. **B)** PTP opening in isolated rat heart mitochondria treated with DMSO (Black line), 1 μM 63 (Green line), 1 μM TR002 (Blue line) or 1 μM CsA (Red line) as monitored by CRC assay. **C)** Data were quantified at different concentrations of the compounds (0.01–10 μM). *p < 0.05, **p < 0.01, ***p < 0.001 vs DMSO. CRC ratio is compound-to-DMSO treated mitochondria CRC ratios. Isolated heart mitochondria from **D, E)** wild type or **F, G)** CyPD-null mice were analyzed for CRC (**D** and **F**) or swelling (**E** and **G**) assays in presence of DMSO as control (Black line), 1 μM 63 (Green line), 1 μM TR002 (Blue line) or 1 μM CsA (Red line). One hundred μg of mitochondria were challenged with a train of 5 μM $CaCl_2$ pulses for CRC experiments or with a single 50 μM $CaCl_2$ pulse (arrow) for swelling. (For interpretation of the references to colour in this figure legend, the reader is referred to the web version of this article.)
Data are expressed as mean ± SEM. n = 6.

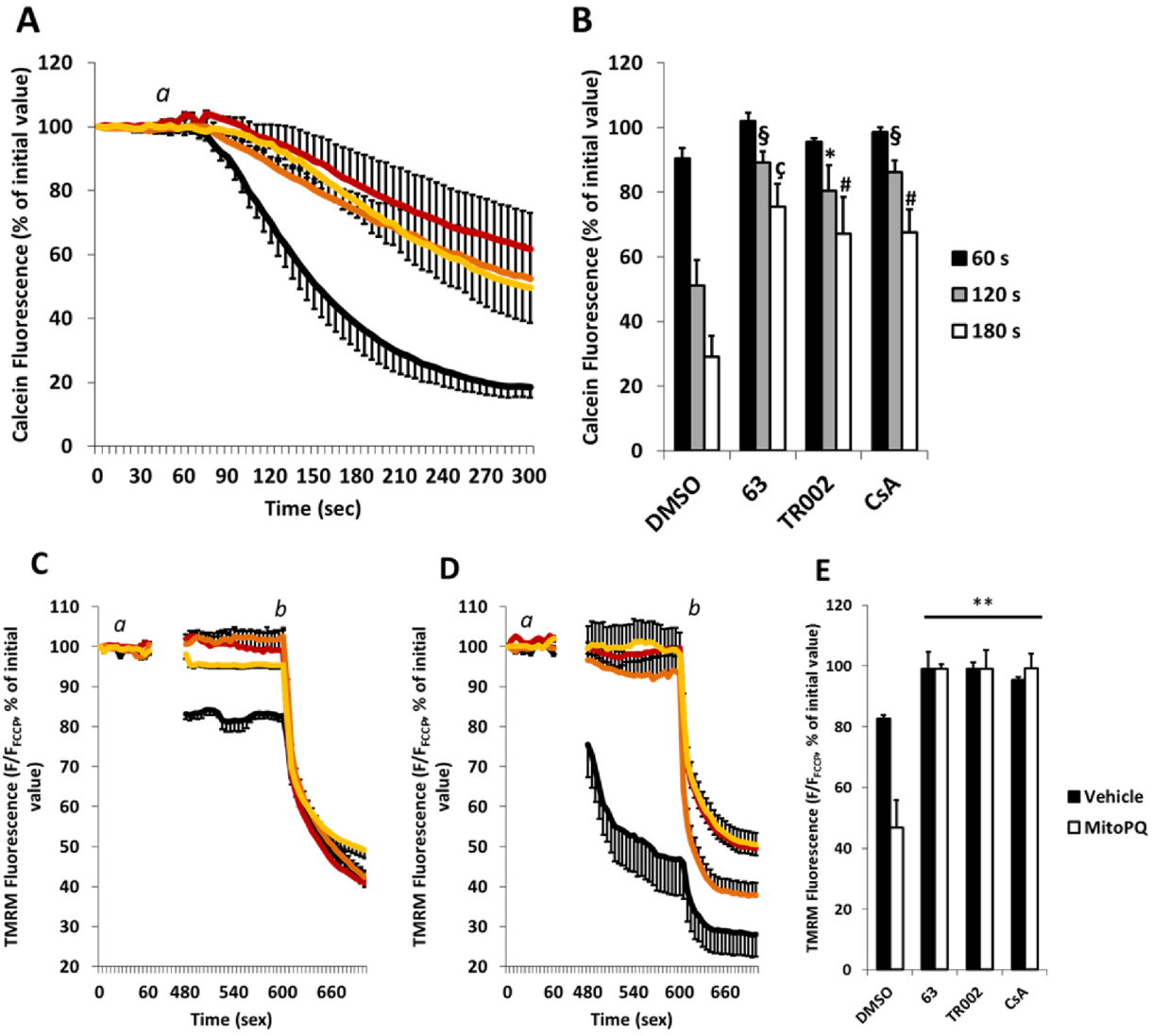

Fig. 2. Effects of compounds 63 and TR002 on PTP opening and mitochondrial membrane potential. A) PTP opening monitored by decrease of calcein fluorescence in isolated NRVMs pretreated for 30 min with DMSO (Black line), 0.5 μM 63 (Red line), 0.5 μM TR002 (Orange line) or 1 μM CsA (Yellow line). a: 5 μM calcimycin. **B)** Data were quantified at different time points after treatment with calcimycin. *p < 0.05, §p < 0.01 vs DMSO 120 s; #p < 0.05, çp < 0.01 vs DMSO 180 s.. **C–D)** Mitochondrial membrane potential (ΔΨm) monitored by TMRM fluorescence in isolated NRVMs following incubation for 1 h with DMSO as control (**C**) or 1 μM MitoPQ (**D**). Cells were pretreated for 30 min with DMSO (Black line), 0.5 μM 63 (Red line), 0.5 μM TR002 (Orange line) or 1 μM CsA (Yellow line). a: 5 μM calcimycin, b: 4 μM FCCP. **E**) Data were quantified after 10 min from the beginning of the experiment and before FCCP injection. **p < 0.01 vs DMSO. Approximately 30 cells were analyzed per condition in each experiment and all the experiments were performed at least three times using three different animal preparations. (For interpretation of the references to colour in this figure legend, the reader is referred to the web version of this article.)
Data are expressed as mean ± SEM.

following 6 h of anoxia, 63 and TR002 preserved Ca^{2+} transients in NRVMs that display a higher number of spontaneous beating cells compared to the control (DMSO: 0 % vs 63: 44.0 ± 15.9 % or TR002: 37.5 ± 19.8 %, Fig. 3F). Indeed, cells treated with either compound did not show significant differences in transient amplitude, frequency and response to caffeine than normoxic control (Fig. 3C–E), while cells treated with DMSO were unexcitable (Fig. 3B). Moreover, NRVMs treated with both 63 and TR002 displayed a preserved response to caffeine (DMSO: 35.2 ± 12.7 % vs 63: 100.0 % or TR002: 93.3 ± 9.4 %, Fig. 3F).

Subsequently, we investigated whether treatment with 63 or TR002 prevents A/R-induced derangements of sarcomeric organization in cardiomyocytes. NRVMs were exposed to 6 h of anoxia followed by 30 min of reoxygenation in the presence or absence of CsA, 63 and TR002, and the distribution of the α-sarcomeric actinin was evaluated by immunocytochemistry. After 6 h of anoxia, NRVMs displayed disrupted sarcomeric structure. In contrast, NRVMs pre-treated with all three compounds displayed a well aligned sarcomeric pattern similar to that observed in normoxic NRVMs (Fig. 4A, Supplementary Fig. 2C). Moreover, the impairment of the mitochondrial morphology observed in DMSO-treated cells was ameliorated in NRVMs treated with the three compounds upon 6 h of anoxic injury (Fig. 4B, Supplementary Fig. 2D).

Since changes in mitochondrial dynamics could be upstream of PTP opening [22,23], expression and distribution of proteins involved in mitochondrial fusion and fission were evaluated in normoxic NRVMs. To this aim, cardiomyocytes were treated in normoxia for 6 h with 1 μM 63 or 1 μM TR002, and their effect was compared with CsA, which is reported to increase DRP1 phosphorylation by inhibiting calcineurin [24]. In contrast to CsA, neither 63 nor TR002 increased DRP1 phosphorylation, (Supplementary Fig. 3A). Furthermore, MFN2 expression levels were not altered by any treatment (Supplementary Fig. 3B). In addition, 63 and TR002 did not modify mitochondrial morphology as evaluated by immunocytochemistry (Supplementary Fig. 3C).

Taken together, our data demonstrate that treatment with either 63

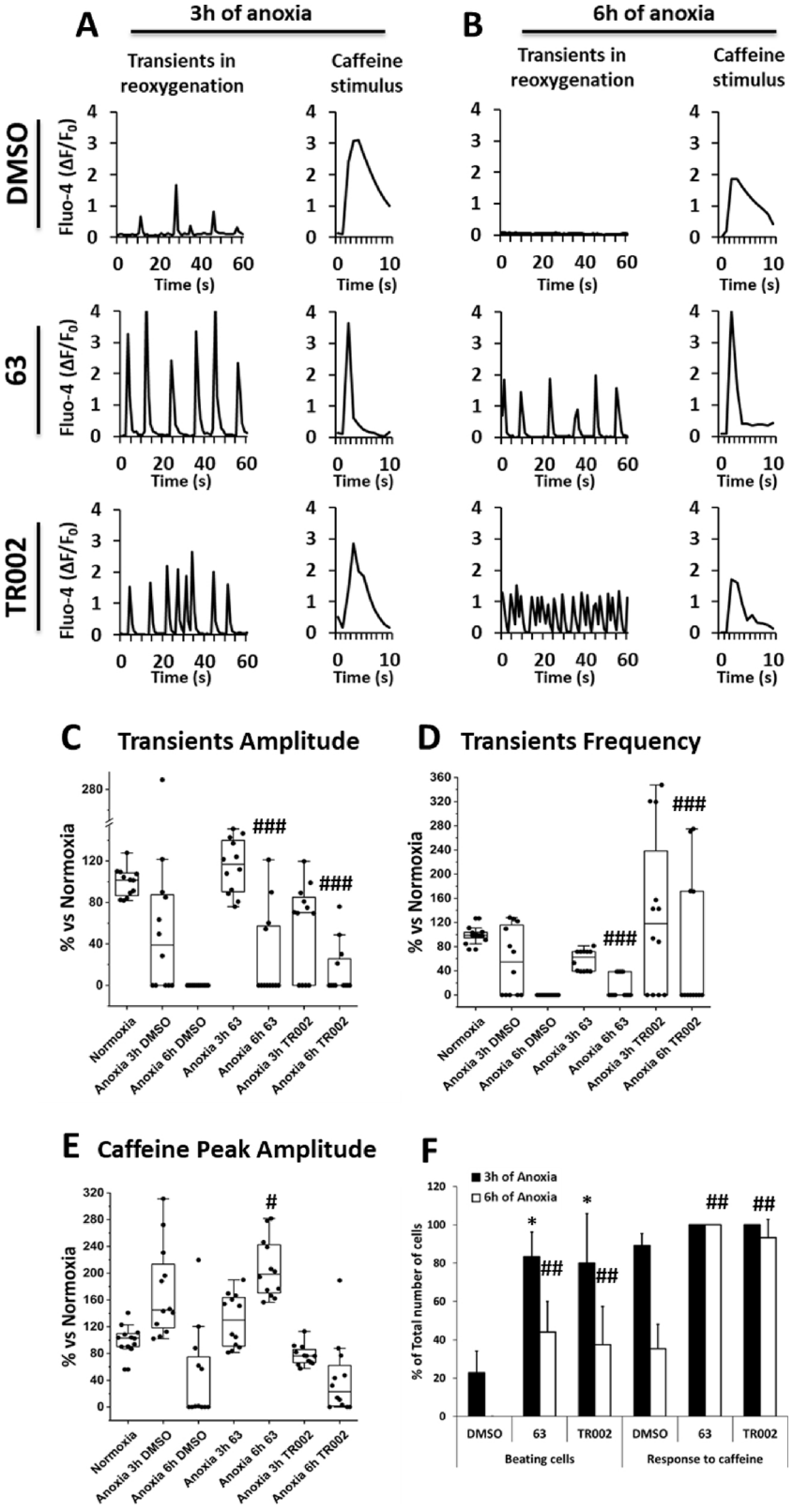

Fig. 3. Effects of compounds 63 and TR002 on cytosolic [Ca^{2+}] homeostasis in NRVMs exposed to A/R. A-E) Cytosolic [Ca^{2+}] homeostasis monitored by Fluo-4 AM in isolated NRVMs treated for 30 min with DMSO, 0.5 μM 63 or 0.5 μM TR002. Cells were exposed either to 3 h and 6 h of anoxia and the Ca^{2+} transients were evaluated during reoxygenation. **A-B**) Comparison between cytosolic Ca^{2+} oscillatory patterns in reoxygenation after (**A**) 3 h or (**B**) 6 h of anoxia. **C**) Transients amplitude average. **D**) Transients frequency average. **E**) Average of caffeine peak amplitude. **F**) Comparison between beating cells and response to caffeine in NRVMs treated with DMSO, 0.5 μM 63 or 0.5 μM TR002 after either 3 h and 6 h of anoxia. **C-E**) #$p < 0.05$, ###$p < 0.001$ vs Anoxia 6 h DMSO. **F**) *$p < 0.05$ vs DMSO 3 h Anoxia; ## $p < 0.01$ vs DMSO 6 h Anoxia. Approximately 20/30 cells were analyzed per condition in each experiment and all the experiments were performed at least three times using three different animal preparations.
Data are expressed as mean ± SEM.

or TR002 preserves mitochondrial function, intracellular [Ca^{2+}] transients and cardiomyocyte contractility in NRVMs following A/R. This protection from A/R injury is associated with the preservation of the mitochondrial morphology and the sarcomeric array in cardiomyocytes. Moreover, the cardioprotective efficacy of both compounds is not contributed by changes in mitochondrial dynamics as might be the case with CsA.

2.4. Compounds 63 and TR002 reduce cardiomyocyte death following anoxia/reoxygenation and protect hearts from ischemic damage

Since PTP opening is one of the main causes of cell death occurring

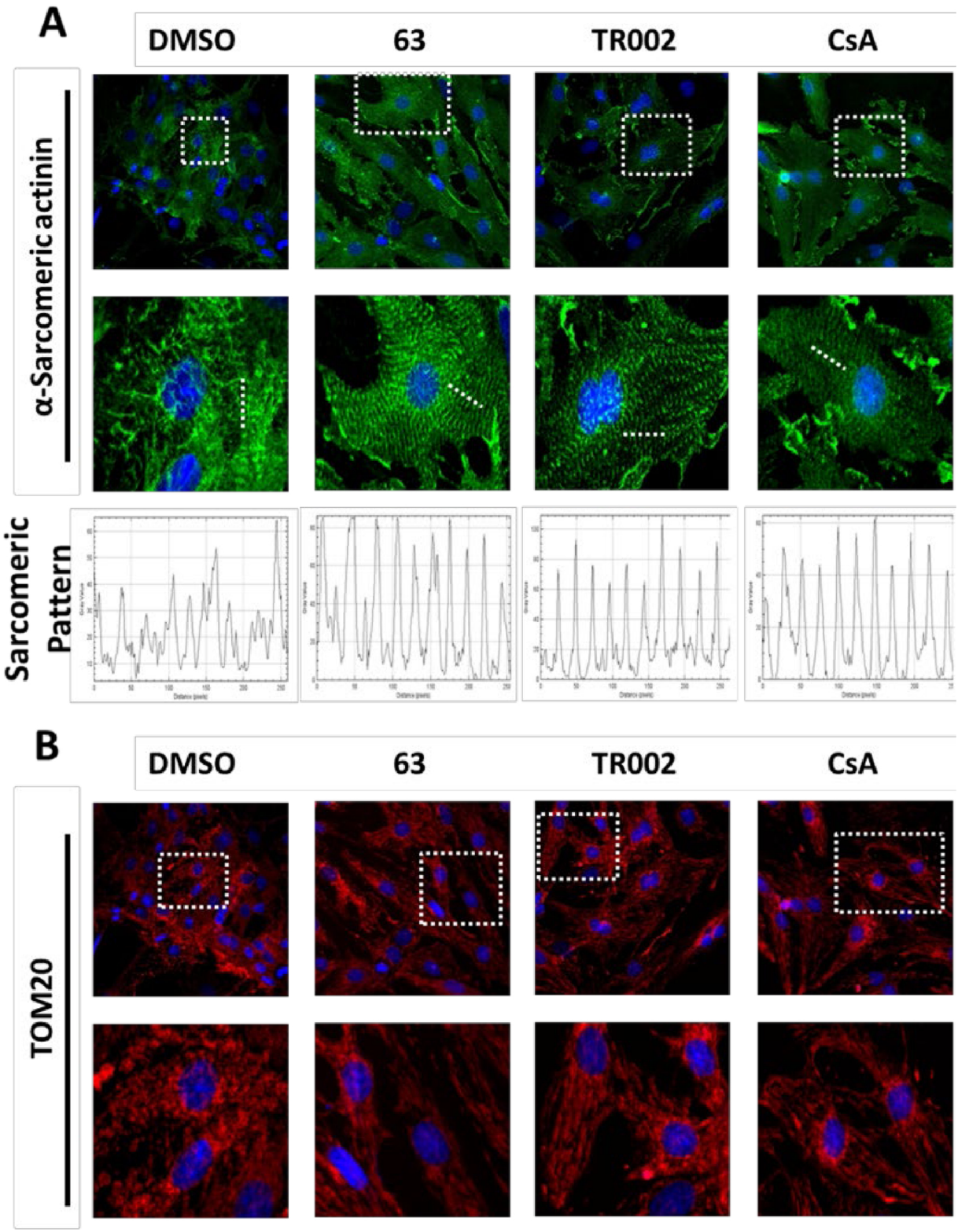

Fig. 4. Effects of compounds 63 and TR002 on sarcomere arrangement and mitochondrial shape. Sarcomere arrangement and **B**) mitochondrial morphology monitored by confocal microscopy in NRVMs exposed to 6 h of anoxia and pretreated for 30 min with DMSO, 0.5 μM **63**, 0.5 μM **TR002** or 1 μM CsA. Confocal images were processed for double immunofluorescent labeling of α-sarcomeric actinin (green) and TOM20 (red). **A)** The fluorescence intensity of α-sarcomeric actinin was plotted and reported on the graph to show the effect of the treatments on the distribution of the sarcomeres within the cell. Both representative images (**A** and **B** upper row) and regions of interests (**A** and **B** lower row) are provided. (For interpretation of the references to colour in this figure legend, the reader is referred to the web version of this article.)

Approximately 20/30 cells were analyzed per condition in each experiment and all the experiments were performed at least three times using three different animal preparations.

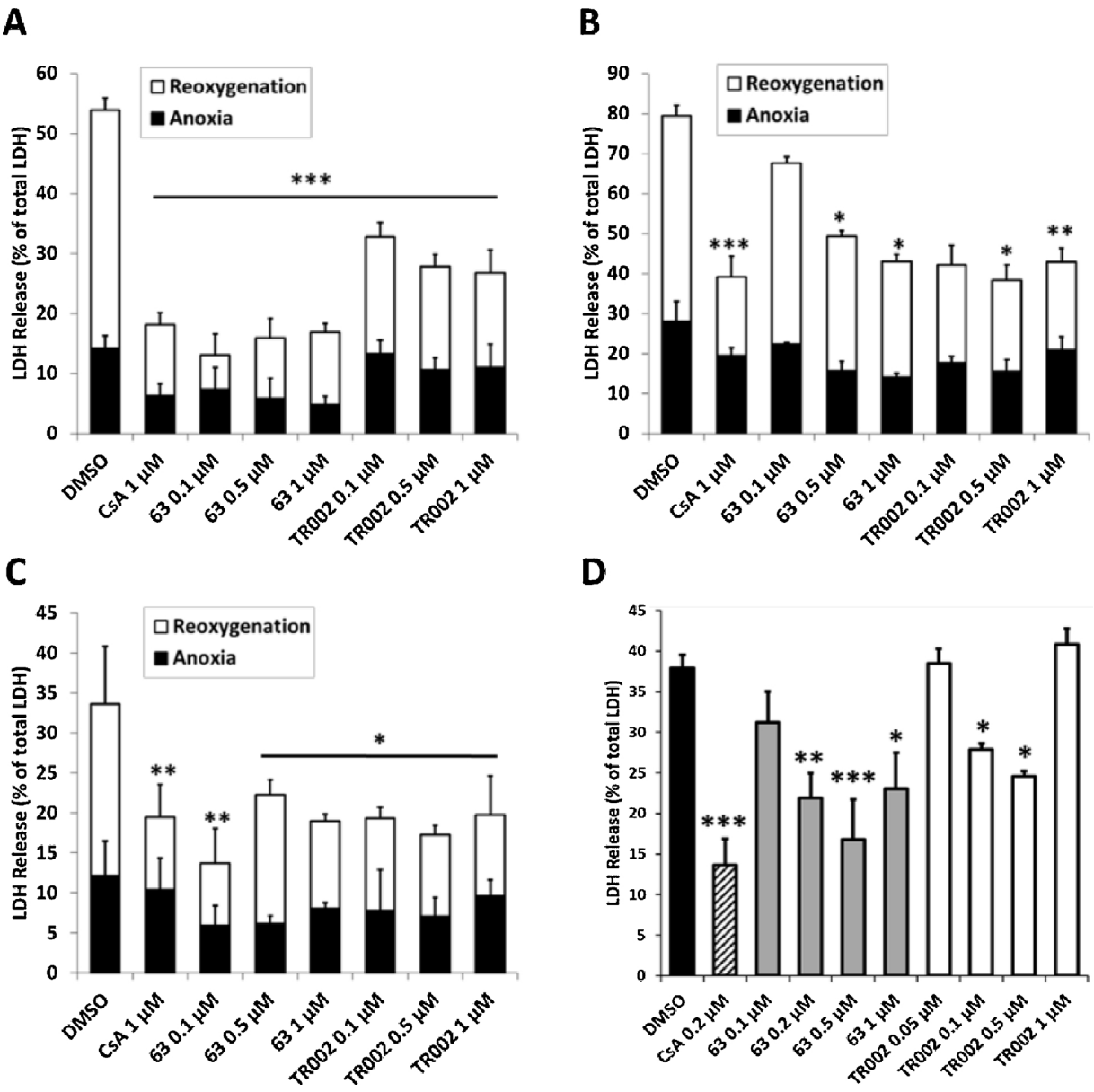

Fig. 5. Effects of compounds 63 and TR002 on cardiomyocytes viability. Cell death measured by LDH release from **A)** isolated NRVMs, **B)** isolated AMVMs and **C)** hiPSc-CMs treated for 30 min with different concentrations of either 63 or TR002 or with 1 µM CsA. *p < 0.05, **p < 0.01, *** p < 0.001 vs DMSO Reoxygenation. **D)** Cell death measured by LDH release in ex vivo hearts perfused in a Langendorff model of I/R, with or without 63, TR002 or CsA. *p < 0.05, **p < 0.01, ***p < 0.001 vs DMSO.
For in vitro experiments (**A, B, C**), approximately 3/4 wells were analyzed per condition in each experiment and all the experiments were performed at least three times using three different animal preparations or cell differentiations. For ex vivo experiments (**D**), n = 5–13.
Data are expressed as mean ± SEM.

during post-ischemic reperfusion (or post-anoxic reoxygenation) [25], we next investigated whether 63 and TR002 could decrease the extent of A/R-induced cardiomyocyte death.

NRVMs, adult mouse ventricular myocytes (AMVMs) and human iPSc-derived cardiomyocytes (hiPSc-CMs) were pre-treated with increasing concentrations of 63 or TR002 (Supplementary Fig. 4A). Similar to CsA, 63 and TR002 at concentrations as low as 0.1 µM protected cardiomyocytes against A/R-induced loss of viability as shown by a decrease in lactate dehydrogenase (LDH) release (Fig. 5). In NRVMs, 63 was more protective than TR002 (Fig. 5A). In AMVMs, higher concentrations (i.e. ≥ 0.5 µM) of 63 and TR002 were required for decreasing cell death (Fig. 5B). Similar to results obtained in NRVMs, all concentrations of 63 and TR002 decreased susceptibility to cell death in hiPSc-CMs (Fig. 5C).

We further examined cardioprotection by 63 or TR002 in isolated mouse hearts perfused at constant flow and subjected to a protocol of I/R. Hearts of 5 month old mice were perfused with different concentrations of 63 or TR002 for 10 min and then subjected to 40 min of ischemia followed by 15 min of reperfusion (Supplementary Fig. 4B). Both 63 and TR002 decreased the release of LDH in a dose-dependent manner up to 0.5 µM (Fig. 5D).

Protective effects were also observed in a different perfusion setup with constant pressure and a latex balloon in the left ventricle for hemodynamic monitoring. The hearts were subjected to 20 min of ischemia followed by 90 min of reperfusion. Hearts were perfused with 0.5 µM of either 63 or TR002 for 10 min prior to ischemia and for the first 10 min of reperfusion (Supplementary Fig. 4B). Treatment with 63 resulted in significantly smaller infarct sizes (DMSO: 65.55 % vs 63:

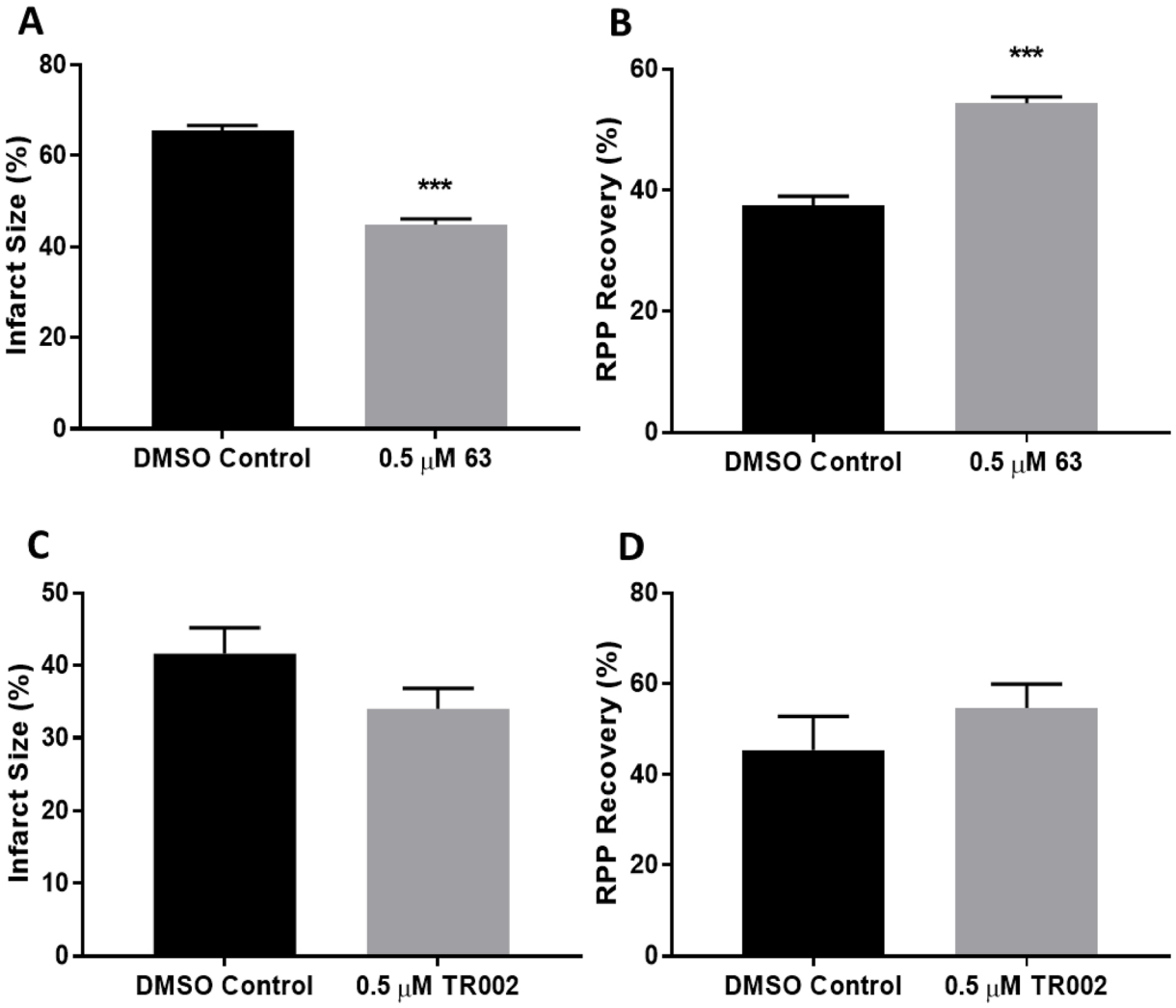

Fig. 6. Effects of compounds 63 and TR002 on functional recovery and cell death by TTC staining. A–C) Cell death measured by TTC staining at 90 min of reperfusion in ex vivo murine hearts perfused in a Langendorff model with a standard I/R procedure after treatment with **A**) 63, and **C**) TR002 compared to DMSO control. **B-D**) Functional recovery calculated by left ventricle developed pressure (LVDP) x heart rate as assessed by intraventricular balloon after treatment with **B**) 63, and **D**) TR002 as compared to DMSO control. *** $p < 0.001$ vs DMSO. $n > 6$.
Data are expressed as mean ± SEM.

44.90 %, $p < 0.001$, Fig. 6A, Supplementary Fig. 4C) and significantly better post-ischemic recovery compared to vehicle-perfused hearts (DMSO: 37.52 % vs 63: 54.35 %, $p < 0.001$, Fig. 6B). Treatment with TR002 trended toward cardioprotection as measured by a decrease in infarct size (DMSO: 41.45 % vs TR002: 33.83 %, $p = 0.120$, Fig. 6C) and an increase in rate pressure product (RPP) recovery (DMSO: 45.38 % vs TR002: 54.60 %, $p = 0.33$, Fig. 6D) but did not reach statistical significance.

Taken together, these results indicate that 63 and TR002 reduce the susceptibility to both anoxic and ischemic injury, both *in vitro* and *ex vivo* by decreasing the opening of the PTP in cardiomyocytes derived from different species. In general, 63 was more cardioprotective than TR002.

3. Discussion

This study shows that our recently-described small-molecule inhibitors of the PTP, isoxazole 63 and triazole TR002, protect against cardiomyocyte injury caused by A/R *in vitro* in isolated cardiomyocytes, and by I/R *ex vivo* in perfused hearts. Notably, the inhibition of PTP opening by 63 and TR002 is independent of CyPD since PTP opening was equally inhibited in mitochondria isolated from WT and *Ppif*$^{-/-}$ mice. Besides reducing the extent of I/R-induced loss of viability, 63 and TR002 maintained mitochondrial function, intracellular [Ca^{2+}] homeostasis, cardiomyocyte contractility and sarcomeric organization.

Previous studies have documented the protective effect of indirect PTP inhibition via targeting of its regulator CyPD with CsA in animal models [6–9]; however, this protection failed to be translated in a human clinical trial [12,13]. Recently, new CyPD-independent, small-molecule inhibitors of the PTP were discovered [14–16]. Here, we show that two of these compounds, 63 and TR002, are more potent than CsA in inhibiting PTP opening in both isolated cardiac mitochondria and cardiomyocytes. Protection against A/R-induced cell death by 63 and TR002 was observed in mouse, rat and human cardiac cells, as well as in *ex vivo* mouse hearts. Besides demonstrating species-independent protective effects, the present findings show the occurrence of protection due to PTP inhibition in human cardiomyocytes. This result represents a relevant pre-requisite for translating our results to the clinics.

The present findings strongly support the critical role of PTP opening in cardiac injury induced by post-ischemic reperfusion. Besides showing improved viability as documented previously [26–28], here we find that inhibition of PTP opening by 63 and TR002 not only maintains mitochondrial function, but also prevents morphological and functional perturbations occurring at the cytosolic level in

cardiomyocytes during reperfusion. Therefore, the disruption of mitochondrial bioenergetics induced by PTP opening is likely to be upstream of the loss of cardiomyocyte function and viability caused by I/R, reinforcing the importance of targeting PTP to obtain a robust cardioprotection.

Previous efforts at PTP inhibition as a therapeutic strategy for cardioprotection focused on the indirect regulator CyPD. However, this approach was not successful in clinical studies [29]. The reason why CsA was not cardioprotective is unclear, but could be due to the fact that CyPD is an indirect regulator of the PTP, and that pore opening can occur also in its absence [30]; alternatively, poor pharmacokinetics of CsA could have contributed to the lack of clinical success [29,30]. In addition, CyPD inhibition has been described to result in detrimental effects, especially exacerbating adverse remodeling of hypertrophied hearts [26,31]. This could be due to an increase in matrix [Ca^{2+}] as a consequence of a decreased occurrence of PTP opening. If this is the case, however, the present compounds could mimic the negative effects of CyPD targeting. A recent study demonstrates that the negative consequence of matrix Ca^{2+} accumulation resulting from the deletion of the mitochondrial Na^+/Ca^{2+} exchanger is prevented by CyPD deletion [32]. Therefore, rather than causing cardiac injury by increased matrix [Ca^{2+}] PTP inhibition appears to prevent cardiac derangements resulting from intra-mitochondrial Ca^{2+} overload. The negative outcome of pharmacological or genetic targeting of CyPD could be related to the loss of its activity and/or interaction with other proteins. Since CyPD is a prolyl isomerase required for the correct folding of intra-mitochondrial proteins, its absence or inhibition could hamper mitochondrial proteostasis [33]. This negative effect is not likely to be generated by CyPD-independent PTP inhibitors.

In any case, additional studies are needed to investigate whether the prolonged administration of the novel PTP inhibitors is devoid of negative effects.

4. Methods

4.1. Cell culture and treatments

Neonatal rat ventricular myocytes (NRVMs) were isolated from 1 to 3 day old Wistar rats as described previously [34]. Cardiomyocytes were plated in 0.1 % porcine gelatin (Sigma) coated plates at variable density (at least 3 × 10^5 cells/ml) in MEM supplemented with 10 % FBS (Thermo Fisher Scientific), 1 % penicillin/streptomycin (Thermo Fisher Scientific), 1 % non-essential amino acids (Thermo Fisher Scientific), 1 mM 5-Bromo-2-Deoxyuridine (Sigma). Cells were maintained at 37 °C in the presence of 5 % CO_2. The medium was changed to MEM supplemented with 1 % FBS, 1 % penicillin/streptomycin and 1 % non-essential amino acids after 24 h of plating.

Adult mouse ventricular myocytes (AMVMs) were isolated from the hearts of 12-week old C57Bl6/*J* mice, as previously described [35]. Collagenase-digested isolated myocytes were incubated in buffer with increasing concentrations of Ca^{2+}, achieving a final concentration of 1.2 mM Ca^{2+} as in DMEM plating media. Cells were seeded at 3 × 10^4 rod-shaped myocytes/well in DMEM plating media supplemented with 10 mM 2,3-Butanedione monoxime (BDM, SIGMA) in 24-well plates coated with laminin. After 1 h incubation at 37 °C, 5 % CO_2, plating media was replaced to remove unattached cells.

Human induced pluripotent stem cells (hiPSc) were differentiated into cardiomyocytes (CMs) by means of the STEMdiff™ Cardiomyocyte Differentiation Kit (Stemcell Technologies) following manufacturer's instructions. Briefly, hiPSc were plated at the density of 3.5 × 10^5 cells/well in a 12-well plate. After reaching 90 % confluence, cells were incubated with the induction medium A for the mesodermal commitment. Two days after, cardiac mesoderm commitment was achieved by the addition of medium B. After four days, the medium was replaced with medium C for the cardiac induction. After eight days from the beginning of the differentiation protocol, the induction medium C was replaced with maintenance medium and cells were re-fed every 48 h. Cells differentiated with this protocol display spontaneous beating usually on Day 7 and robust contracting syncytium by Day 10. On Day 20, beating cardiomyocytes have been selected as described before [36]. Briefly, cells were cultured in Glucose-free DMEM (no glucose, no pyruvate, Life Technologies) supplemented with 4 mM Na-DL-Lactate (Sigma) for 48 h. Medium was renewing every day and it was replaced after 2 days with maintenance medium. Cardiomyocytes were used for the experiments after 4 days from the selection protocol.

To evaluate the effect of the compounds, cells were pre-treated with different concentrations of either 63 and TR002, from 0.1 to 1 μM, for 30 min unless specified in Section 3. Moreover, to prevent PTP opening cells were pre-treated with 1 μM CsA (Sigma) [4] for 30 min as control.

4.2. Tissue mitochondria isolation

Cardiac mitochondria were isolated from Sprague Dawley rats (2–3 months old), control mice (C57BL/6 wild type mice) and mice lacking the *Ppif* gene which encodes for CyPD (*Ppif*$^{-/-}$ mice) which have been described previously [37]. Mouse heart mitochondria were isolated in mouse heart mitochondria (MHM) buffer (in mM: 225 mannitol, 75 sucrose, 10 HEPES-Tris and 1 EGTA, pH 7.4) as described before [4]. Briefly, hearts were rapidly excised, rinsed with cold MHM to remove blood and cut into small pieces. These were re-suspended into 1 ml of MHM supplemented with 0.1 mg/ml Nagarse (Sigma) and homogenized with a pre-chilled glass-Teflon homogenizer for 3 min. Then 6 ml of MHM supplemented with 0.2 % BSA were added to stop Nagarse action and homogenate was spun at 500 *g* for 10 min at 4 °C. Supernatant was filtered through a 150 μm mesh, transferred into a new tube and spun at 10,000*g* for 10 min at 4 °C. Pellet was resuspended in MHM buffer, spun at 7500 *g* for 6 min at 4 °C and washed again with MHM. After another centrifuge at 7500 *g* for 6 min pellet was re-suspended in 100 μl MHM and stored on ice. Protein quantification was determined with BCA method.

Mouse liver mitochondria were isolated in MS-EGTA buffer (in mM: 225 mannitol, 75 sucrose, 5 HEPES, and 1 EGTA, pH 7.4, Sigma). Tissues were minced into 2 mm X 2 mm pieces and then homogenized using a glass and teflon tissue homogenizer (8 strokes) on ice and in MS-EGTA buffer. Tissue homogenates were then subjected to an 800 *g* centrifugation for 5 min (1X) and the supernatants were then centrifuged at 10,000*g* for 10 min. Isolated mitochondria were then suspended in KCl buffer (in mM: 125 KCl, 20 HEPES, 2 $MgCl_2$, 2 KH_2PO_4, and 0.04 EGTA, pH 7.2, Sigma) for subsequent assays.

All experimental procedures with animals conducted at the Cincinnati Children's Medical Center were approved by the Institutional Animal Care and Use Committee of Cincinnati Children's Medical Center, protocols IACUC 2018-0047. We have complied with the relevant ethical considerations for animal usage overseen by this committee. The number of mice used in this study reflects the minimum number needed to achieve statistical significance based on experience and previous power analysis. Both sexes of mice were used in equal ratios.

4.3. Assessment of calcium retention capacity (CRC) and mitochondrial swelling assays

CRC was determined using Calcium Green-5 N (Invitrogen), a low affinity membrane-impermeant probe that increases its fluorescence emission upon Ca^{2+} binding. Just prior to initiation of the assay, mitochondrial suspension was spun at 9500 *g* for 5 min at 4 °C to remove EGTA, supernatant was then discarded and the pellet suspended at 0.25 mg/ml in a buffer containing 250 mM sucrose, 10 mM MOPS-Tris, 1 mM Pi-Tris, 10 μM EGTA-Tris, 5 mM glutamate-Tris, 2.5 mM malate-Tris and 0.5 μM Calcium Green-5 N, pH 7.4. Mitochondrial suspension was then dispensed to wells of black 96-well plate (final volume 0.2 ml) and subjected to trains of 5 μM (mouse mitochondria) or 10 μM (rat

mitochondria) Ca^{2+} pulses followed by 3 s linear shaking and fluorescence (ex/em = 485/535) read for 4 min with Tecan Infinite F200 plate reader. Experiments were performed at 25 °C.

The CRC assay and the mitochondrial swelling assay in *Ppif*$^{-/-}$ liver mitochondria were performed simultaneously using a dual-detector (one to measure fluorescence and the other to measure absorbance) single-cuvette based fluorimeteric system (Horiba Scientific). Isolated mitochondria (2 mg) were loaded into the cuvette along with 0.25 μM Calcium Green-5 N (Invitrogen), 7 mM pyruvate (Sigma), and 1 mM malate (Sigma) and brought up to 1 ml using KCl buffer (as described above). Mitochondria were then pulsed with sequential additions of 100 μM $CaCl_2$ until PTP opening occurred or until the mitochondria reached a $CaCl_2$ saturation point and could no longer take up more Ca^{2+}.

4.4. Live imaging

Experiments using NRVMs were carried out in HBSS at pH 7.4 (adjusted with NaOH) and at 37 °C.

Images were acquired using an inverted fluorescence microscope (Leica DMI6000B equipped with DFC365FX camera) with PL APO 40x/1.25 oil objective. Fluorescence intensity was quantified using the Fiji distribution of the Java-based image processing program ImageJ [38], and background signal was subtracted from all analyzed regions of interest. For Ca^{2+} imaging, traces were analyzed using the "Peak Analyzer" tool of Origin Pro 9.1.

To monitor mitochondrial membrane potential (ΔΨm), cells were incubated with 25 nM tetramethylrhodamine (Thermo Fisher Scientific) in presence of 1.6 μM cyclosporin H for 30 min at 37 °C in a humidified incubator. Tetramethylrhodamine fluorescence intensity was monitored following addition of 4 μM oligomycin (Sigma) and images were acquired before and after the addition of 4 μM carbonyl cyanide-*p*-trifluoromethoxyphenylhydrazone (Sigma) [34]. PTP opening was induced by 5 μM of the Ca^{2+} ionophore calcimycin, in presence or absence of 1 μM MitoParaquat that evokes a primary increase in mitochondrial ROS [21].

To monitor PTP opening, cells were incubated with 1 μM calcein acetoxymethyl (AM) ester (Thermo Fisher Scientific) in presence of 2 mM Cobalt Chloride ($CoCl_2$) for 15 min at 37 °C in a humidified incubator followed by 20 min of de-esterification as previously described [17].

To monitor $[Ca^{2+}]_I$ homeostasis, cells were incubated with 5 μM Fluo-4 acetoxymethyl (AM) ester (Thermo Fisher Scientific), 0.01 % w/v pluronic F-127 (Sigma) and 250 μM sulfinpyrazone (Sigma), for 20 min at 37 °C in a humidified incubator followed by 20 min of de-esterification. The experiments were performed in normoxia and after both 3 h and 6 h of anoxia followed by 30 min of reoxygenation.

4.5. Immunocytochemistry

NRVMs were prepared for staining by means of Cardiomyocyte Immunocytochemistry Kit (Thermo Fisher Scientific) following manufacturer's instruction. Briefly, NRVMs were fixed with Fixative Solution for 30 min, permeabilized with Permeabilization Solution S for 15 min at room temperature and then blocked with Blocking Solution for 30 min. Mitochondria were stained using anti-TOM20 antibody (Santa Cruz; 1:500, rabbit) and sarcomeres were stained using anti-α-sarcomeric actinin antibody (Sigma; 1:500, mouse) over-night at 4 °C. The day after, samples were incubated with Alexa Fluor 594 conjugated anti-rabbit (Life Technologies, 1:250) and Alexa Fluor 488 conjugated anti-mouse (Life Technologies, 1:250) for 1 h at room temperature. Coverslips were mounted using NucBlue™ Fixed Cell ReadyProbes™ Reagent with DAPI to stain nuclei (Invitrogen). Images were collected at Zeiss LSM 700 confocal system equipped with a PlanApo 40x/1.2 oil objective, and an Argon laser used to excite the fluorophores at the appropriate wavelength. Images were collected at 2048 × 2048 pixels per image with a 100 Hz acquisition rate. Images were analyzed using the Fiji distribution of the Java-based image processing program ImageJ [38]. The experiments were performed both in normoxia and after 6 h of anoxia followed by 30 min of reoxygenation.

4.6. Western blot analysis

NRVMs were plated in 12-well plates at density of 4 × 10^5 cells/well. Five days after, cells were incubated for 6 h in HBSS supplemented with DMSO, 1 μM 63, 1 μM TR002 or 1 μM CsA. NRVMs were homogenized in RIPA Lysis Buffer (1X, EMD Millipore) containing protease (1X, cOmplete mini protease inhibitor cocktail, Roche) and phosphatase (1X, PhosStop, Roche) inhibitors. Protein concentration was determined using BCA protein assay (BCA Kit, Euroclone). Proteins were separated using 4–12 % Bis-Tris gels (Life Technologies) in MES/SDS running buffer 1X (i.e. 1 M MES, 1 M Tris Base, 69.3 mM SDS, 20.5 mM EDTA, pH 7.3). Proteins were transferred to nitrocellulose membrane (Bio-Rad) by western blot in transfer buffer (i.e. 250 mM Tris Base, 1.92 M glycine, 0.1 % SDS) over-night (O/N) at 4 °C. Membranes were blocked for 1 h with 5 % BSA in TBS-Tween, and incubated O/N with the following primary antibodies diluted in 5 % BSA:

- Anti p-DRP1 (Ser637) → 1:1000 (Cell Signaling, #4867, rabbit)
- Anti DRP1 →1:1000 (BD Biosciences, #611738, mouse)
- Anti MFN2 →1:1000 (Abnova, #H00009927-M03, mouse)
- Anti ATP Synthase subunit β →1:1000 (Abcam, #14730, mouse)

Following incubation with primary antibodies, membranes were washed three times in TBS-Tween, 5 min each, and incubated for 1 h with the following secondary antibodies diluted in 5 % BSA:

- Anti mouse (m-IgGκ BP-HRP) →1:3000 (Santa Cruz Biotechnology, #sc-516102)
- Anti rabbit (mouse anti-rabbit IgG-HRP) →1:3000 (Santa Cruz Biotechnology, #sc-2357)

Following incubation with primary and secondary HRP-conjugated antibodies, bands were detected by the PierceTM ECL Western Blotting Substrate using the UVITEC Cambridge, mini HD instrument. The results were expressed as densitometry analysis performed using the Fiji distribution of the Java-based image processing program ImageJ [38].

4.7. Assessment of cell death in vitro

For anoxia/reoxygenation experiments, NRVMs and hiPSc-CMs were seeded in 24-well plates at density of 1.5 × 10^5 cells/well and incubated in (in mM) 118 NaCl, 5 KCl, 1.2 KH_2PO_4, 1.2 $MgSO_4$, 2 $CaCl_2$, 25 MOPS at pH 6.4 during anoxia or pH 7.4 during reoxygenation, while AMVMs were seeded in 24-wells plates at density of 3 × 10^4 cells/well and incubated in (in mM) 118 NaCl, 5 KCl, 1.2 KH_2PO_4, 1.2 $MgSO_4$, 2 $CaCl_2$, 10 HEPES, 4 $NaHCO_3$, supplemented with 25 μM Blebbistatin (Sigma) at pH 6.4 during anoxia or pH 7.4 during reoxygenation [39]. Anoxia was induced adding 10 mM 2-deoxy-D-glucose and incubating in a BD GasPak™ EZ Anaerobe Gas-generating Pouch System with an indicator (BD Biosciences) at 37 °C. NRVMs were exposed to anoxia for 12 h, hiPSc-CMs were exposed to anoxia for 10 h, and AMVMs were exposed to anoxia for 8 h [40]. To induce reoxygenation, plates were removed from the GasPak™ pouch, 2-deoxy-D-glucose was replaced with 10 mM D-glucose, the pH was restored at 7.4. The plates were then incubated in a humidified incubator at 37 °C (i.e. 4 h NRMVs, 4 h hiPsc-CMs, 10 h AMVMs). A schematic description of the protocol applied *in vitro* is reported in Supplementary Fig. 4A.

The release of lactate dehydrogenase (LDH) from cardiomyocytes was measured to evaluate cell death occurring in normoxia, anoxia and reoxygenation as described before [4,41]. Supernatant aliquots were collected after both anoxia and reoxygenation. At the end of every

experiment, intact cells were lysed by incubating with 1 % Triton X-100 (Sigma) for 30 min and supernatants were collected to evaluate the total amount of LDH. LDH enzymatic activity was measured spectrophotometrically by the absorbance of nicotinamide adenine dinucleotide (Roche) at 340 nm, indicative of the reduction of pyruvate to lactate.

4.8. Assessment of cell death ex vivo

In one series of studies, hearts were subjected to ischemia/reperfusion (I/R) using a non-recirculating Langendorff model at constant flow [42,43] with a bicarbonate buffer (in mM: 118.5 NaCl, 3.1 KCl, 1.18 KH_2PO_4, 25 $NaHCO_3$, 1.2 $MgCl_2$, 1.4 $CaCl_2$, and 11 D-glucose, pH 7.4) insufflated with 95 % O_2 – 5 % CO_2 at 37 °C, supplemented with different concentrations of DMSO, CsA, 63, or TR002 (Supplementary Fig. 4B). For LDH measurements, the hearts were rapidly excised from cervical-dislocated 5 months' sex-matched C57BL/6 J mice and perfused retrogradely for 20 min at a constant flux of 5 ml/min. The hearts were subjected to 40 min of global no-flow ischemia, and 15 min of reperfusion. Coronary effluent during the reperfusion period was collected every minute to measure LDH. At the end of reperfusion, the hearts were quickly homogenized in 0.5 % Triton X-100 for total LDH measurement. Since all values were normalized to heart weight, the amount of LDH release was expressed as % of total LDH (i.e. effluent + homogenate) to rule out possible changes due to variations in heart size [4].

All experiments conducted at the National Institutes of Health received humane treatment in accordance with National Institutes of Health guidelines and the "Guiding Principles for Research Involving Animals and Human Beings". This portion of the study was reviewed and approved by the Institutional Animal Care and Use Committee of the National Heart, Lung, and Blood Institute. In experiments testing hemodynamic recovery and infarct size, the hearts were excised from 12-16-week-old C57BL/6 N (Taconic Farms, USA) mice under pentobarbital anaesthesia and perfused retrogradely at 100 cm of water at 37 °C (Supplementary Fig. 4B) as previously described [44,45]. Both heart rate (HR) and left ventricular developed pressure (LVDP) were measured using a latex balloon connected to a pressure transducer and inserted into the left ventricle. Data was recorded and digitized using a PowerLab system (ADInstruments, Colorado Springs, CO). The rate-pressure product (RPP = LVDP X heart rate) was used as an index of cardiac contractile function. RPP recovery is presented as a percent recovery at the end of reperfusion as compared to baseline perfusion. For measurement of myocardial infarct size, at the end of the 90 min of reperfusion, hearts were perfused with 1 % (wt/vol) of 2,3,5-triphenyltetrazolium chloride (TTC) and incubated in TTC at 37 °C for 30 min, followed by fixation in 10 % (wt/vol) formaldehyde. Infarct size was expressed as the percentage of the total cross-sectional area of the heart.

4.9. Data analysis

All values are expressed as mean ± S.E.M. Comparison between groups was performed by one-way ANOVA, followed by a Tukey's post hoc multiple comparison where data were normally distributed. Data that did not follow the normal distribution were statistically analysed by Kolgomorov-Smirnov's test. Comparisons between two groups were performed using a two-tailed Student's t-test. A value of $p < 0.05$ was considered significant.

Author contributions

EM, FDL, PB, MF, MO and JDM conceived the study. JS, MJB and MC designed and performed experiments on isolated mitochondria. SA, MDS and PA designed and performed experiments on isolated cells. TB and RM designed and performed experiments on ex vivo hearts. JD and MC synthesized isoxazole 63 and triazole TR002. SA, MDS, JS, MJB, MP, FDL, MC, PB, MF and EM wrote the manuscript.

Declaration of Competing Interest

None.

Acknowledgements

This work was supported by the Leducq Transatlantic Network of Excellence 16CVD04, the COST Action EU-CARDIOPROTECTION CA16225, the Grant number MSM200111701 provided by the Czech Academy of Sciences. TMB was supported by the NIH Medical Research Scholars Program, a public-private partnership supported jointly by the NIH and contributions to the Foundation for the NIH from the Doris Duke Charitable Foundation, the American Association for Dental Research, the Colgate-Palmolive Company, and other private donors.

Appendix A. Supplementary data

Supplementary material related to this article can be found, in the online version, at doi:https://doi.org/10.1016/j.phrs.2019.104548.

References

[1] T.A. Gaziano, Cardiovascular disease in the developing world and its cost-effective management, Circulation 112 (23) (2005) 3547–3553.
[2] D.R. Hunter, R.A. Haworth, J.H. Southard, Relationship between configuration, function, and permeability in calcium-treated mitochondria, J. Biol. Chem. 251 (16) (1976) 5069–5077.
[3] R. Assaly, A. de Tassigny, S. Paradis, S. Jacquin, A. Berdeaux, D. Morin, Oxidative stress, mitochondrial permeability transition pore opening and cell death during hypoxia-reoxygenation in adult cardiomyocytes, Eur. J. Pharmacol. 675 (1–3) (2012) 6–14.
[4] F. Di Lisa, R. Menabo, M. Canton, M. Barile, P. Bernardi, Opening of the mitochondrial permeability transition pore causes depletion of mitochondrial and cytosolic NAD+ and is a causative event in the death of myocytes in postischemic reperfusion of the heart, J. Biol. Chem. 276 (4) (2001) 2571–2575.
[5] X. Liu, G. Hajnoczky, Altered fusion dynamics underlie unique morphological changes in mitochondria during hypoxia-reoxygenation stress, Cell Death Differ. 18 (10) (2011) 1561–1572.
[6] G. Ikeda, T. Matoba, Y. Nakano, K. Nagaoka, A. Ishikita, K. Nakano, D. Funamoto, K. Sunagawa, K. Egashira, Nanoparticle-mediated targeting of cyclosporine a enhances cardioprotection against ischemia-reperfusion injury through inhibition of mitochondrial permeability transition pore opening, Sci. Rep. 6 (2016) 20467.
[7] S.Y. Lim, S.M. Davidson, D.J. Hausenloy, D.M. Yellon, Preconditioning and postconditioning: the essential role of the mitochondrial permeability transition pore, Cardiovasc. Res. 75 (3) (2007) 530–535.
[8] M. Paillard, L. Gomez, L. Augeul, J. Loufouat, E.J. Lesnefsky, M. Ovize, Postconditioning inhibits mPTP opening independent of oxidative phosphorylation and membrane potential, J. Mol. Cell. Cardiol. 46 (6) (2009) 902–909.
[9] C. Weinbrenner, G.S. Liu, J.M. Downey, M.V. Cohen, Cyclosporine A limits myocardial infarct size even when administered after onset of ischemia, Cardiovasc. Res. 38 (3) (1998) 676–684.
[10] T. Nakagawa, S. Shimizu, T. Watanabe, O. Yamaguchi, K. Otsu, H. Yamagata, H. Inohara, T. Kubo, Y. Tsujimoto, Cyclophilin D-dependent mitochondrial permeability transition regulates some necrotic but not apoptotic cell death, Nature 434 (7033) (2005) 652–658.
[11] D.J. Hausenloy, E.A. Boston-Griffiths, D.M. Yellon, Cyclosporin A and cardioprotection: from investigative tool to therapeutic agent, Br. J. Pharmacol. 165 (5) (2012) 1235–1245.
[12] T.T. Cung, O. Morel, G. Cayla, G. Rioufol, D. Garcia-Dorado, D. Angoulvant, E. Bonnefoy-Cudraz, P. Guerin, M. Elbaz, N. Delarche, P. Coste, G. Vanzetto, M. Metge, J.F. Aupetit, B. Jouve, P. Motreff, C. Tron, J.N. Labeque, P.G. Steg, Y. Cottin, G. Range, J. Clerc, M.J. Claeys, P. Coussement, F. Prunier, F. Moulin, O. Roth, L. Belle, P. Dubois, P. Barragan, M. Gilard, C. Piot, P. Colin, F. De Poli, M.C. Morice, O. Ider, J.L. Dubois-Rande, T. Unterseeh, H. Le Breton, T. Beard, D. Blanchard, G. Grollier, V. Malquarti, P. Staat, A. Sudre, E. Elmer, M.J. Hansson, C. Bergerot, I. Boussaha, C. Jossan, G. Derumeaux, N. Mewton, M. Ovize, Cyclosporine before PCI in patients with acute myocardial infarction, N. Engl. J. Med. 373 (11) (2015) 1021–1031.
[13] F. Ottani, R. Latini, L. Staszewsky, L. La Vecchia, N. Locuratolo, M. Sicuro, S. Masson, S. Barlera, V. Milani, M. Lombardi, A. Costalunga, N. Mollichelli, A. Santarelli, N. De Cesare, P. Sganzerla, A. Boi, A.P. Maggioni, U. Limbruno, C. Investigators, Cyclosporine A in reperfused myocardial infarction: the multicenter, controlled, open-label CYCLE trial, J. Am. Coll. Cardiol. 67 (4) (2016) 365–374.
[14] S. Roy, J. Sileikyte, M. Schiavone, B. Neuenswander, F. Argenton, J. Aube,

M.P. Hedrick, T.D. Chung, M.A. Forte, P. Bernardi, F.J. Schoenen, Discovery, synthesis, and optimization of diarylisoxazole-3-carboxamides as potent inhibitors of the mitochondrial permeability transition pore, ChemMedChem 10 (10) (2015) 1655–1671.
[15] S. Roy, J. Sileikyte, B. Neuenswander, M.P. Hedrick, T.D. Chung, J. Aube, F.J. Schoenen, M.A. Forte, P. Bernardi, N-Phenylbenzamides as potent inhibitors of the mitochondrial permeability transition pore, ChemMedChem 11 (3) (2016) 283–288.
[16] J. Sileikyte, J. Devereaux, J. de Jong, M. Schiavone, K. Jones, A. Nilsen, P. Bernardi, M. Forte, M. Cohen, Second generation inhibitors of the mitochondrial permeability transition pore with improved plasma stability, ChemMedChem 14 (20) (2019) 1771–1782.
[17] V. Petronilli, G. Miotto, M. Canton, M. Brini, R. Colonna, P. Bernardi, F. Di Lisa, Transient and long-lasting openings of the mitochondrial permeability transition pore can be monitored directly in intact cells by changes in mitochondrial calcein fluorescence, Biophys. J. 76 (2) (1999) 725–734.
[18] F. Di Lisa, P. Bernardi, Mitochondria and ischemia-reperfusion injury of the heart: fixing a hole, Cardiovasc. Res. 70 (2) (2006) 191–199.
[19] N. Zamzami, P. Marchetti, M. Castedo, T. Hirsch, S.A. Susin, B. Masse, G. Kroemer, Inhibitors of permeability transition interfere with the disruption of the mitochondrial transmembrane potential during apoptosis, FEBS Lett. 384 (1) (1996) 53–57.
[20] M. Dietel, I. Herzig, A. Reymann, I. Brandt, B. Schaefer, A. Bunge, H.J. Heidebrecht, A. Seidel, Secondary combined resistance to the multidrug-resistance-reversing activity of cyclosporin A in the cell line F4-6RADR-CsA, J. Cancer Res. Clin. Oncol. 120 (5) (1994) 263–271.
[21] E.L. Robb, J.M. Gawel, D. Aksentijevic, H.M. Cocheme, T.S. Stewart, M.M. Shchepinova, H. Qiang, T.A. Prime, T.P. Bright, A.M. James, M.J. Shattock, H.M. Senn, R.C. Hartley, M.P. Murphy, Selective superoxide generation within mitochondria by the targeted redox cycler MitoParaquat, Free Radic. Biol. Med. 89 (2015) 883–894.
[22] S.B. Ong, S. Subrayan, S.Y. Lim, D.M. Yellon, S.M. Davidson, D.J. Hausenloy, Inhibiting mitochondrial fission protects the heart against ischemia/reperfusion injury, Circulation 121 (18) (2010) 2012–2022.
[23] S.B. Ong, A.R. Hall, R.K. Dongworth, S. Kalkhoran, A. Pyakurel, L. Scorrano, D.J. Hausenloy, Akt protects the heart against ischaemia-reperfusion injury by modulating mitochondrial morphology, Thromb. Haemost. 113 (3) (2015) 513–521.
[24] G.M. Cereghetti, A. Stangherlin, O. Martins de Brito, C.R. Chang, C. Blackstone, P. Bernardi, L. Scorrano, Dephosphorylation by calcineurin regulates translocation of Drp1 to mitochondria, Proc. Natl. Acad. Sci. U. S. A. 105 (41) (2008) 15803–15808.
[25] F. Di Lisa, M. Canton, A. Carpi, N. Kaludercic, R. Menabo, S. Menazza, M. Semenzato, Mitochondrial injury and protection in ischemic pre- and post-conditioning, Antioxid. Redox Signal. 14 (5) (2011) 881–891.
[26] F. Di Lisa, P. Bernardi, Modulation of mitochondrial permeability transition in ischemia-reperfusion injury of the heart. Advantages and limitations, Curr. Med. Chem. 22 (20) (2015) 2480–2487.
[27] J.Q. Kwong, J.D. Molkentin, Physiological and pathological roles of the mitochondrial permeability transition pore in the heart, Cell Metab. 21 (2) (2015) 206–214.
[28] R.J. Parks, E. Murphy, J.C. Liu, Mitochondrial permeability transition pore and calcium handling, Methods Mol. Biol. 1782 (2018) 187–196.
[29] L. Monassier, E. Ayme-Dietrich, G. Aubertin-Kirch, A. Pathak, Targeting myocardial reperfusion injuries with cyclosporine in the CIRCUS trial – pharmacological reasons for failure, Fundam. Clin. Pharmacol. 30 (2) (2016) 191–193.
[30] P. Bernardi, F. Di Lisa, Cyclosporine before PCI in acute myocardial infarction, N. Engl. J. Med. 374 (1) (2016) 89–90.
[31] J.W. Elrod, R. Wong, S. Mishra, R.J. Vagnozzi, B. Sakthievel, S.A. Goonasekera, J. Karch, S. Gabel, J. Farber, T. Force, J.H. Brown, E. Murphy, J.D. Molkentin, Cyclophilin D controls mitochondrial pore-dependent Ca(2+) exchange, metabolic flexibility, and propensity for heart failure in mice, J. Clin. Invest. 120 (10) (2010) 3680–3687.
[32] T.S. Luongo, J.P. Lambert, P. Gross, M. Nwokedi, A.A. Lombardi, S. Shanmughapriya, A.C. Carpenter, D. Kolmetzky, E. Gao, J.H. van Berlo, E.J. Tsai, J.D. Molkentin, X. Chen, M. Madesh, S.R. Houser, J.W. Elrod, The mitochondrial Na(+)/Ca(2+) exchanger is essential for Ca(2+) homeostasis and viability, Nature 545 (7652) (2017) 93–97.
[33] V. Giorgio, M.E. Soriano, E. Basso, E. Bisetto, G. Lippe, M.A. Forte, P. Bernardi, Cyclophilin D in mitochondrial pathophysiology, Biochim. Biophys. Acta 1797 (6–7) (2010) 1113–1118.
[34] N. Kaludercic, A. Carpi, T. Nagayama, V. Sivakumaran, G. Zhu, E.W. Lai, D. Bedja, A. De Mario, K. Chen, K.L. Gabrielson, M.L. Lindsey, K. Pacak, E. Takimoto, J.C. Shih, D.A. Kass, F. Di Lisa, N. Paolocci, Monoamine oxidase B prompts mitochondrial and cardiac dysfunction in pressure overloaded hearts, Antioxid. Redox Signal. 20 (2) (2014) 267–280.
[35] T.D. O'Connell, M.C. Rodrigo, P.C. Simpson, Isolation and culture of adult mouse cardiac myocytes, Methods Mol. Biol. 357 (2007) 271–296.
[36] S. Tohyama, F. Hattori, M. Sano, T. Hishiki, Y. Nagahata, T. Matsuura, H. Hashimoto, T. Suzuki, H. Yamashita, Y. Satoh, T. Egashira, T. Seki, N. Muraoka, H. Yamakawa, Y. Ohgino, T. Tanaka, M. Yoichi, S. Yuasa, M. Murata, M. Suematsu, K. Fukuda, Distinct metabolic flow enables large-scale purification of mouse and human pluripotent stem cell-derived cardiomyocytes, Cell Stem Cell 12 (1) (2013) 127–137.
[37] C.P. Baines, R.A. Kaiser, N.H. Purcell, N.S. Blair, H. Osinska, M.A. Hambleton, E.W. Brunskill, M.R. Sayen, R.A. Gottlieb, G.W. Dorn, J. Robbins, J.D. Molkentin, Loss of cyclophilin D reveals a critical role for mitochondrial permeability transition in cell death, Nature 434 (7033) (2005) 658–662.
[38] J. Schindelin, I. Arganda-Carreras, E. Frise, V. Kaynig, M. Longair, T. Pietzsch, S. Preibisch, C. Rueden, S. Saalfeld, B. Schmid, J.Y. Tinevez, D.J. White, V. Hartenstein, K. Eliceiri, P. Tomancak, A. Cardona, Fiji: an open-source platform for biological-image analysis, Nat. Methods 9 (7) (2012) 676–682.
[39] J.M. Bond, B. Herman, J.J. Lemasters, Protection by acidotic pH against anoxia/reoxygenation injury to rat neonatal cardiac myocytes, Biochem. Biophys. Res. Commun. 179 (2) (1991) 798–803.
[40] R. Matsuoka, K. Ogawa, H. Yaoita, W. Naganuma, K. Maehara, Y. Maruyama, Characteristics of death of neonatal rat cardiomyocytes following hypoxia or hypoxia-reoxygenation: the association of apoptosis and cell membrane disintegrity, Heart Vessels 16 (6) (2002) 241–248.
[41] H.U. Bergmeyer, E. Bernt, Methods of Enzymatic Analysis, Verlag Chemie, Weinheim, Germany, 1974.
[42] L. Iop, E. Dal Sasso, R. Menabo, F. Di Lisa, G. Gerosa, The rapidly evolving concept of whole heart engineering, Stem Cells Int. 2017 (2017) 8920940.
[43] J. Sileikyte, E. Blachly-Dyson, R. Sewell, A. Carpi, R. Menabo, F. Di Lisa, F. Ricchelli, P. Bernardi, M. Forte, Regulation of the mitochondrial permeability transition pore by the outer membrane does not involve the peripheral benzodiazepine receptor (Translocator Protein of 18 kDa (TSPO)), J. Biol. Chem. 289 (20) (2014) 13769–13781.
[44] J. Sun, A.M. Aponte, S. Menazza, M. Gucek, C. Steenbergen, E. Murphy, Additive cardioprotection by pharmacological postconditioning with hydrogen sulfide and nitric oxide donors in mouse heart: S-sulfhydration vs. S-nitrosylation, Cardiovasc. Res. 110 (1) (2016) 96–106.
[45] Y. Guo, M.P. Flaherty, W.J. Wu, W. Tan, X. Zhu, Q. Li, R. Bolli, Genetic background, gender, age, body temperature, and arterial blood pH have a major impact on myocardial infarct size in the mouse and need to be carefully measured and/or taken into account: results of a comprehensive analysis of determinants of infarct size in 1,074 mice, Basic Res. Cardiol. 107 (5) (2012) 288.

SUPPLEMENTARY FIGURES

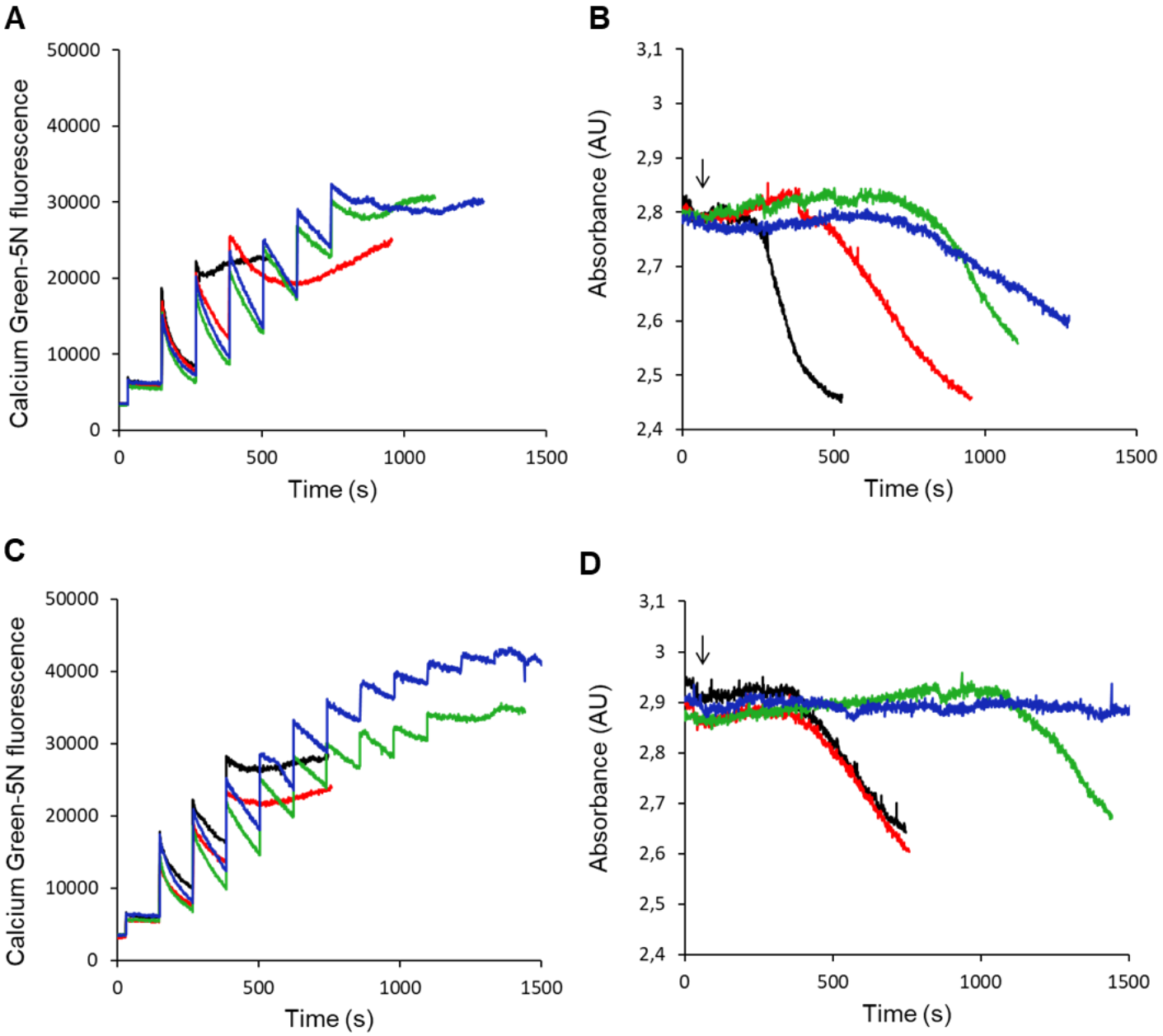

Supplementary Figure 1. Effects of compounds 63 and TR002 on PTP opening in isolated liver mitochondria. A) PTP opening in isolated liver mitochondria from **A, B**) wyldtype or **C, D**) CypD-null mice. Mitochondria were treated with DMSO as control (Black line), 1 µM **63** (Green line), 1 µM **TR002** (Blue line) or 1 µM CsA (Red line) as monitored by simultaneous CRC (**A** and **C**) and swelling (**B** and **D**) assay. Control and CyPD-null experiments were conducted concurrently and are only plotted separately for clarity.

Presented data are representative of three independent experiments.

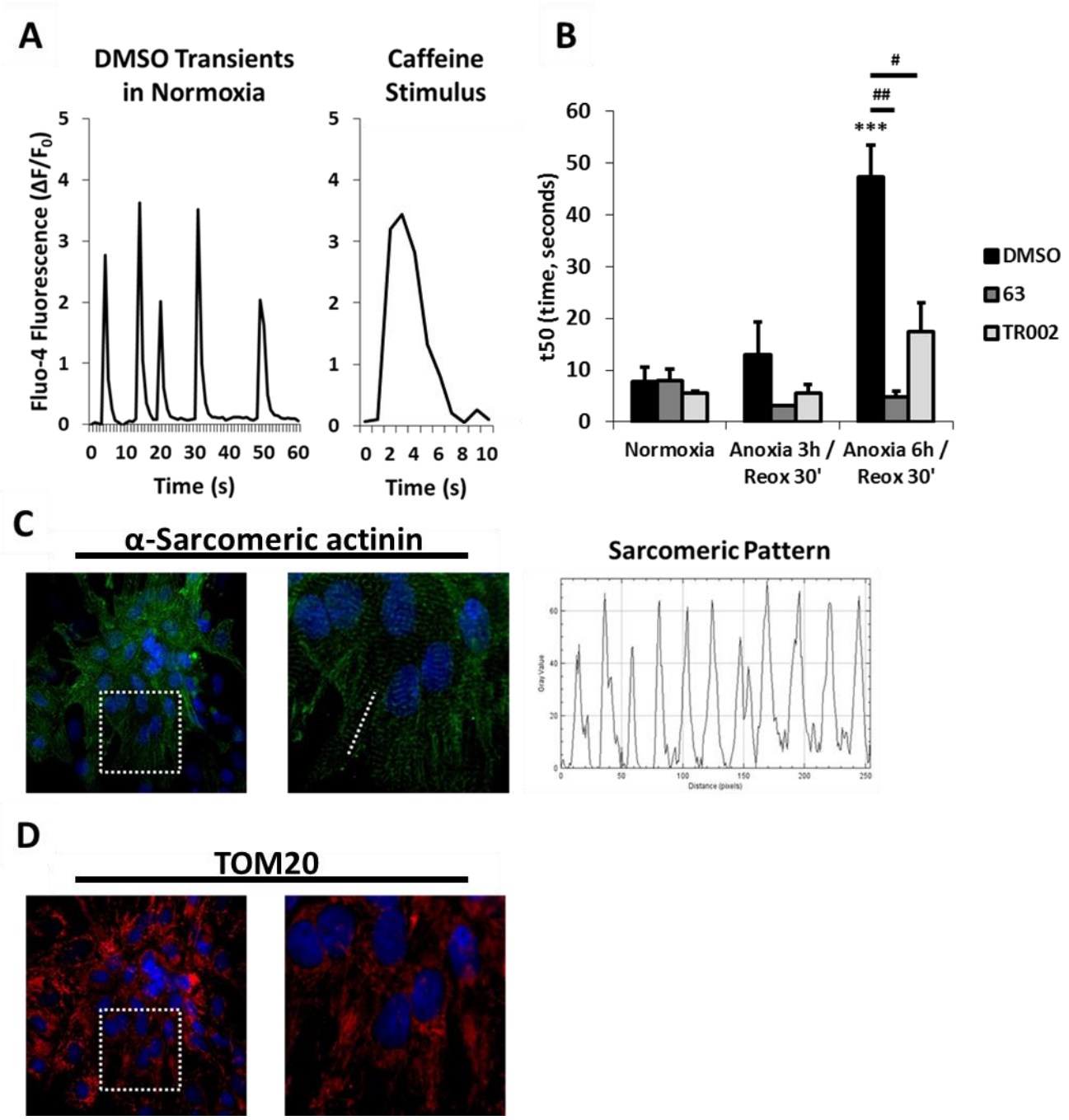

<u>Supplementary Figure 2. Cytosolic [Ca^{2+}] homeostasis, sarcomeres arrangement and mitochondrial shape in normoxic NRVMs.</u> A) Cytosolic [Ca^{2+}] homeostasis monitored by Fluo-4 AM in isolated NRVMs treated for 30 min with DMSO as control in Normoxia. **B)** t50 of caffeine peak in NRVMs treated with **63**, **TR002** or DMSO as control, both before and after anoxic stimulus. **C)** Sarcomeres arrangement and **D**) mitochondrial morphology monitored by confocal microscopy in NRVMs treated for 30 min with DMSO as control in Normoxia. Confocal images were processed for double immunofluorescent labeling of α-sarcomeric actinin (green) and TOM20 (red). Both representative images (**C** and **D** left figure) and regions of interests (**C** and **D** right figure) are provided.

C) The fluorescence intensity of the α-sarcomeric actinin was plotted and reported on the graph to show the distribution of the sarcomeres within the cell in normoxia.

Approximately 20/30 cells were analyzed per condition in each experiment and all the experiments were performed at least three times using three different animal

A


DMSO
63
TR002
CsA
p-DRP1 S637
DRP1 TOT

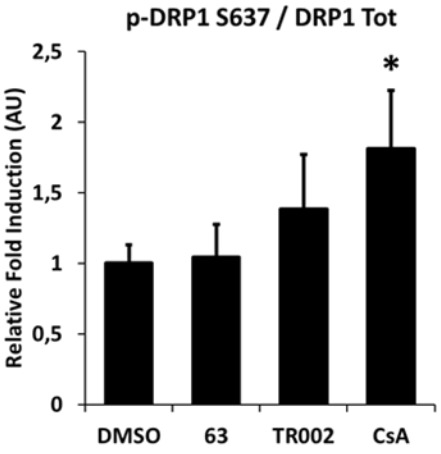
p-DRP1 S637 / DRP1 Tot
Relative Fold Induction (AU)
2,5
2
1,5
1
0,5
0
*
DMSO
63
TR002
CsA

B

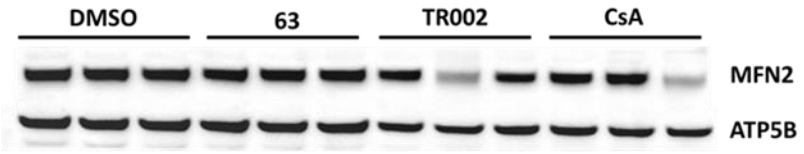
DMSO
63
TR002
CsA
MFN2
ATP5B

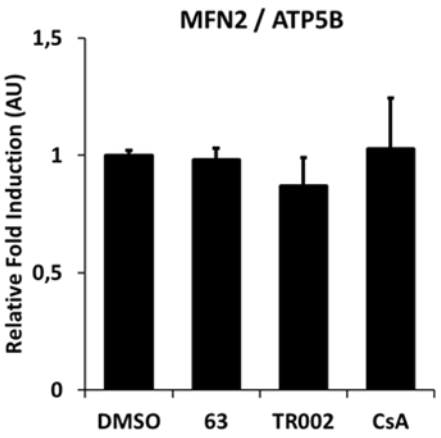
MFN2 / ATP5B
Relative Fold Induction (AU)
1,5
1
0,5
0
DMSO
63
TR002
CsA

C

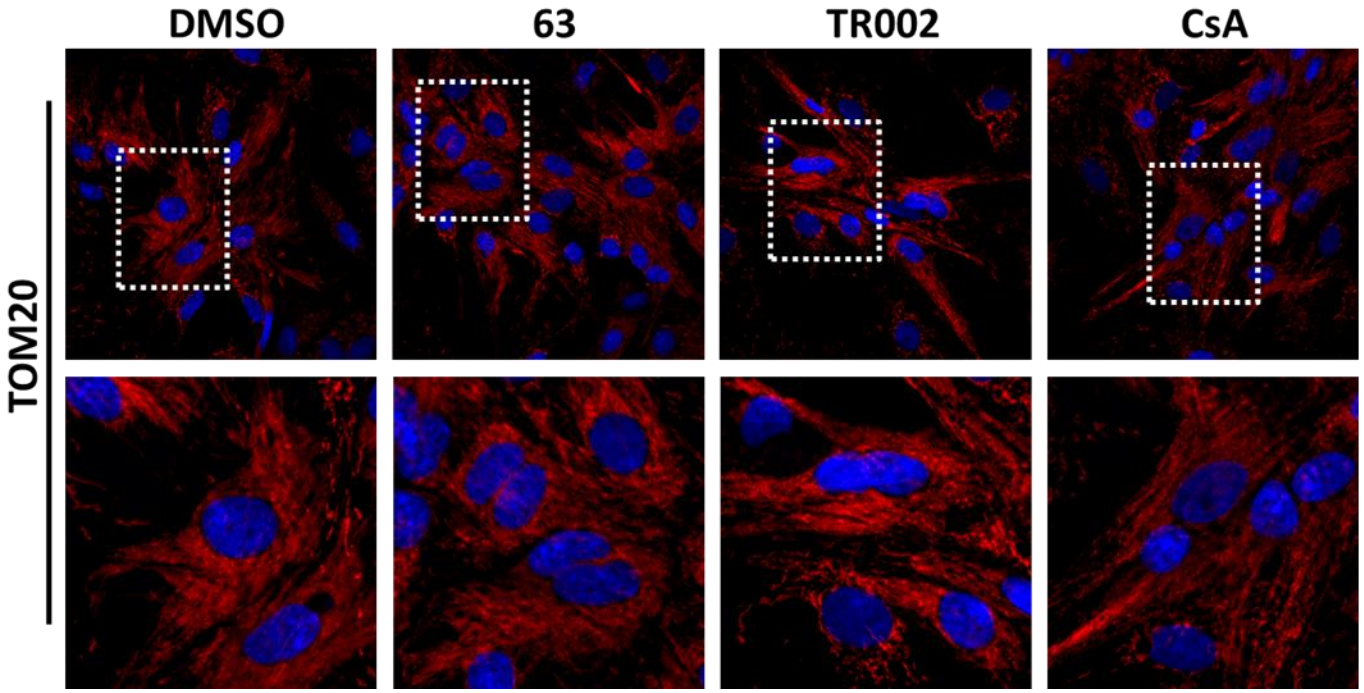
DMSO
63
TR002
CsA
TOM20

Supplementary Figure 3. Effects of compounds 63 and TR002 on mitochondrial shape and dynamics in normoxic NRVMs. **A)** Representative western blot and quantification of DRP1 phosphorylation at S637 in normoxic NRVMs treated for 6h with DMSO, 1 µM 63, 1 µM TR002 or 1 µM CsA. Data were normalized to total DRP1 expression level. Data are expressed as mean ± SEM. *$p < 0.05$ vs DMSO. **B)** Representative western blot and quantification of MFN2 expression level in normoxic NRVMs treated for 6h with DMSO, 1 µM 63, 1 µM TR002 or 1 µM CsA. Data were normalized to ATP Synthase subunit β (ATP5B) level. Data are expressed as mean ± SEM. **C)** Mitochondrial morphology monitored by confocal microscopy in NRVMs treated for 6h with DMSO, 1 µM 63, 1 µM TR002 or 1 µM CsA. Confocal images were processed for immunofluorescent labeling of TOM20 (red). Both representative images (upper row) and regions of interests (lower row) are provided.

Approximately 20/30 cells were analyzed per condition in each experiment and all the experiments were performed at least three times using three different animal preparations.

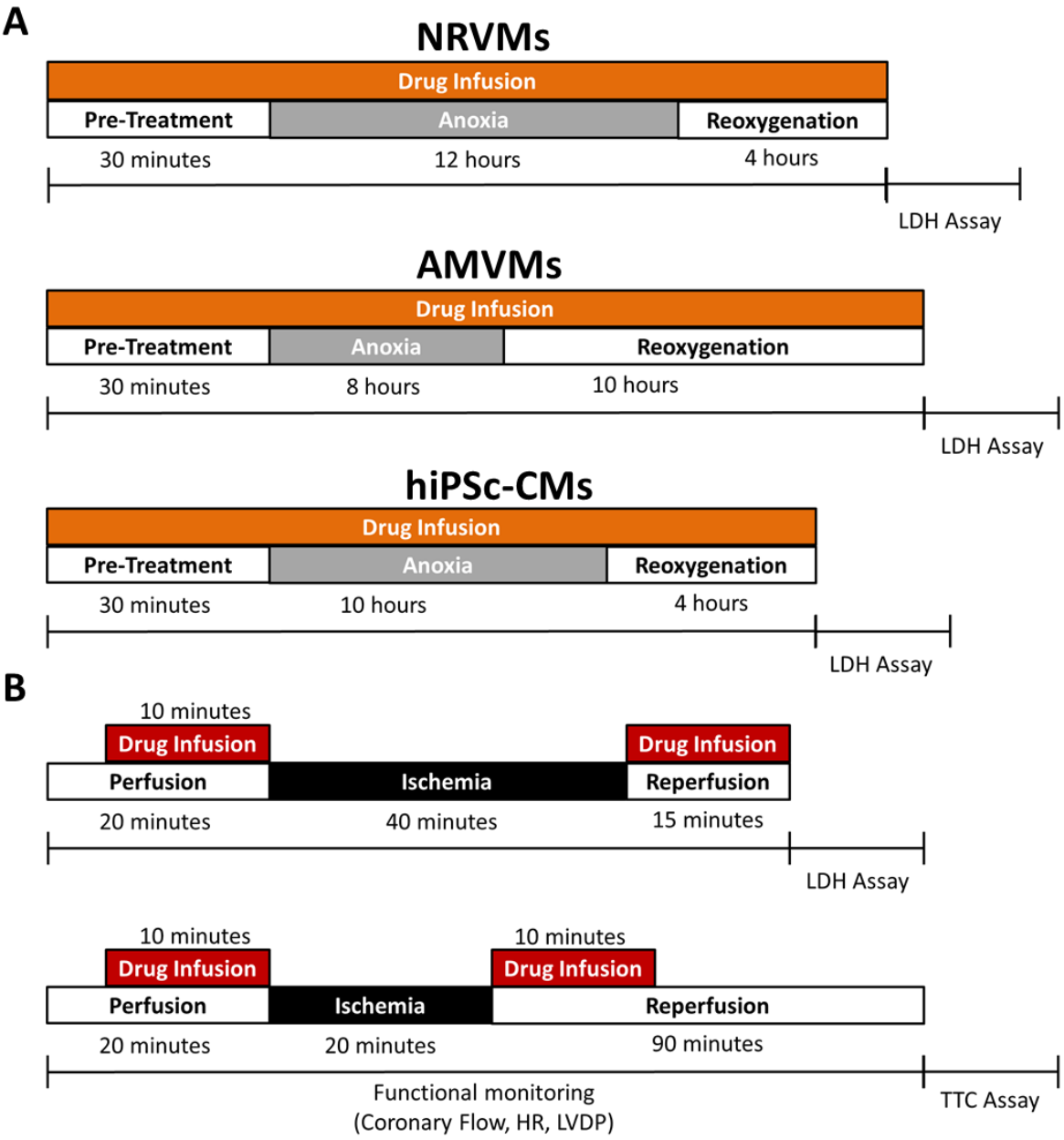
A
NRVMs
Drug Infusion
Pre-Treatment
Anoxia
Reoxygenation
30 minutes
12 hours
4 hours
LDH Assay
AMVMs
Drug Infusion
Pre-Treatment
Anoxia
Reoxygenation
30 minutes
8 hours
10 hours
LDH Assay
hiPSc-CMs
Drug Infusion
Pre-Treatment
Anoxia
Reoxygenation
30 minutes
10 hours
4 hours
LDH Assay
B
10 minutes
Drug Infusion
Drug Infusion
Perfusion
Ischemia
Reperfusion
20 minutes
40 minutes
15 minutes
LDH Assay
10 minutes
10 minutes
Drug Infusion
Drug Infusion
Perfusion
Ischemia
Reperfusion
20 minutes
20 minutes
90 minutes
Functional monitoring
(Coronary Flow, HR, LVDP)
TTC Assay

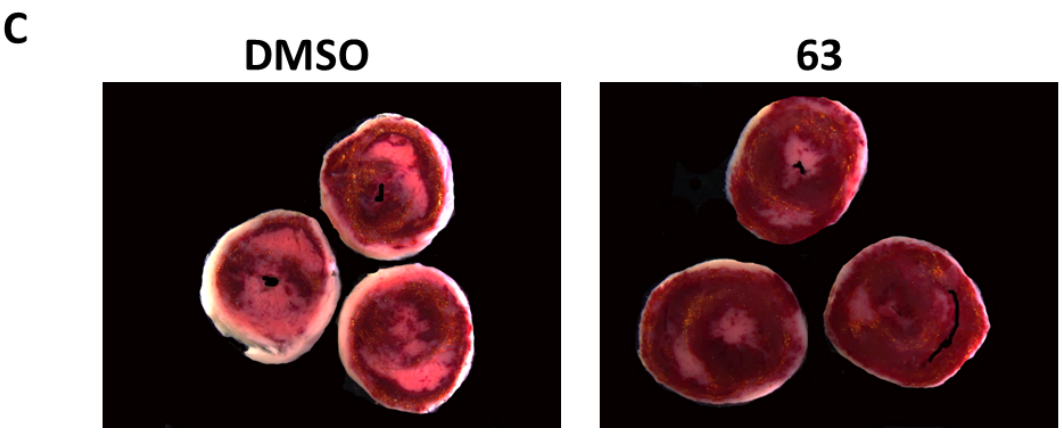
C
DMSO
63

<u>Supplementary Figure 4. Assessment of cell death *in vitro* and *ex vivo.*</u> **A)** Schematic representation of the protocol applied *in vitro* to evaluate the cardioprotection elicited by compounds 63 and TR002 against A/R in NRVMs, AMVMs and hiPSc-CMs. **B)** Schematic representation of the protocol applied *ex vivo* to evaluate the cardioprotection elicited by compounds 63 and TR002 against I/R. **C)** Representative infarct size slices of perfused hearts treated with DMSO or 63 and exposed to I/R. Infarct size was evaluated by TTC staining.